E913/914 Collaboration

Baryon and Hyperon Spectroscopy with the Crystal Ball at Brookhaven National Laboratory

Abilene Christian University - A. Barker, C. Bircher, B. Draper, C. Carter, M. Daugherity, S. Hayden, J. Huddleston, D. Isenhower, J. Qualls, C. Robinson, M. Sadler

Argonne National Laboratory - C. Allgower and H. Spinka

Arizona State University - J. Comfort, K. Craig* and A. Ramirez*

Brookhaven National Laboratory - T. Kycia†

University of California at Los Angeles - M. Clajus, A. Marusic, S. McDonald, B.Nefkens, N. Phaisangittisakul*, S. Prakhov, A. Starostin* and B. Tippens

University of Colorado - J. Peterson

George Washington University - W. Briscoe and A. Shafi*

Universität Karlsruhe - H. Staudenmaier

Kent State University - J.Olmsted* and M. Manley

University of Maryland - D. Peaslee

Petersburg Nuclear Physics Institute - V. Abaev, V. Bekrenev, N. Kozlenko*, S. Kruglov, A. Kulbardis, I. Lopatin and A. Starostin*

University of Regina - N. Knecht*, G. Lolos and Z. Papandreou
G. Huber

Rudjer Boskovic Institute - I. Supek

Valparaiso University - Ak Gibson, D. Grosnick, D. D. Koetke, R. Manweiler and S. Stanislaus

Experiment Spokespersons
* Thesis Students
† Deceased


8/19/2000

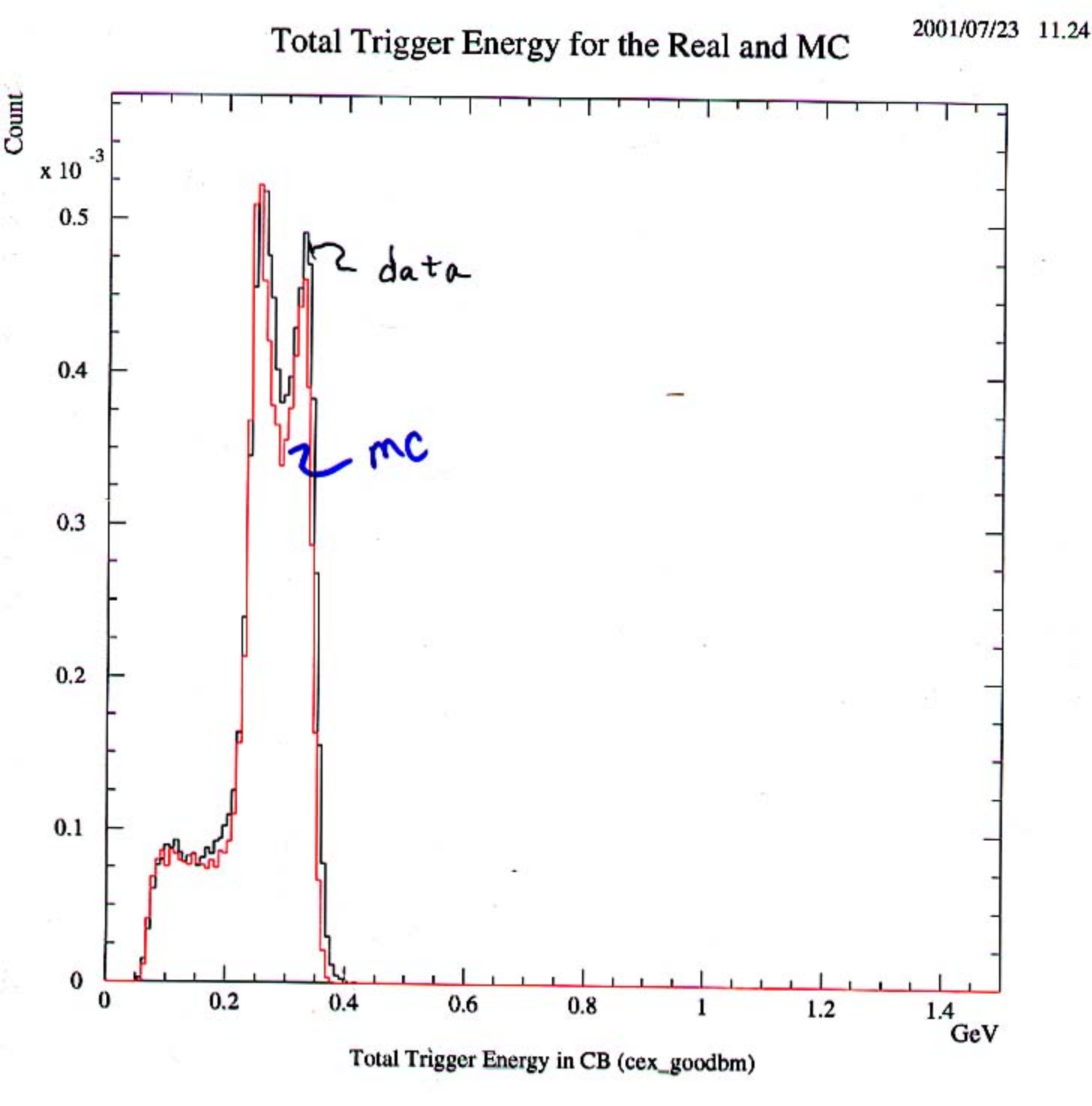
Total Trigger Energy for the Real and MC
2001/07/23 11.24
Count
x 10 -3
0.5
0.4
0.3
0.2
0.1
0
data
mc
0
0.2
0.4
0.6
0.8
1
1.2
1.4
GeV
Total Trigger Energy in CB (cex_goodbm)

2001/07/23 11.33

π^0 Invariant Mass Peak for Real and MC

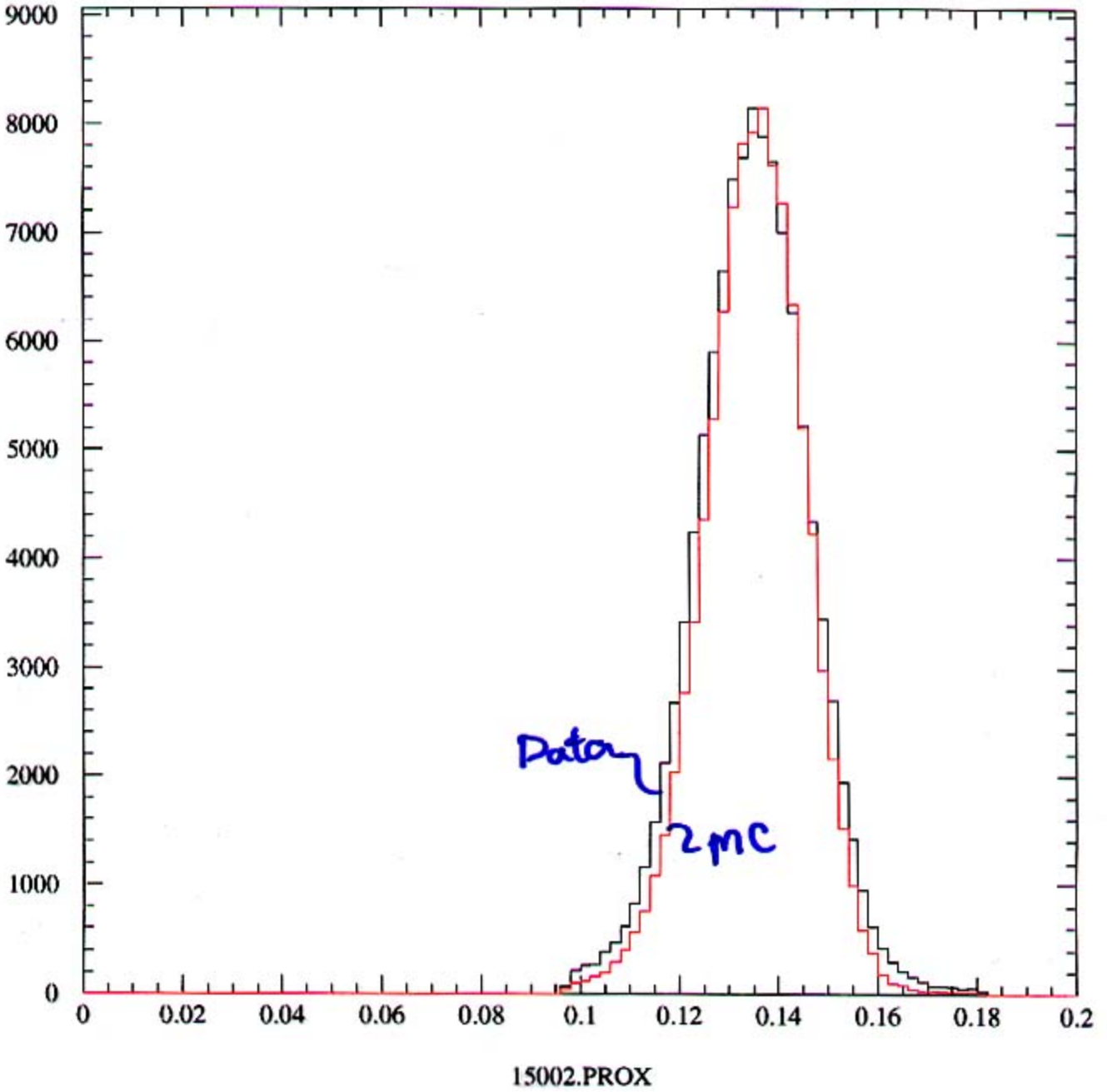

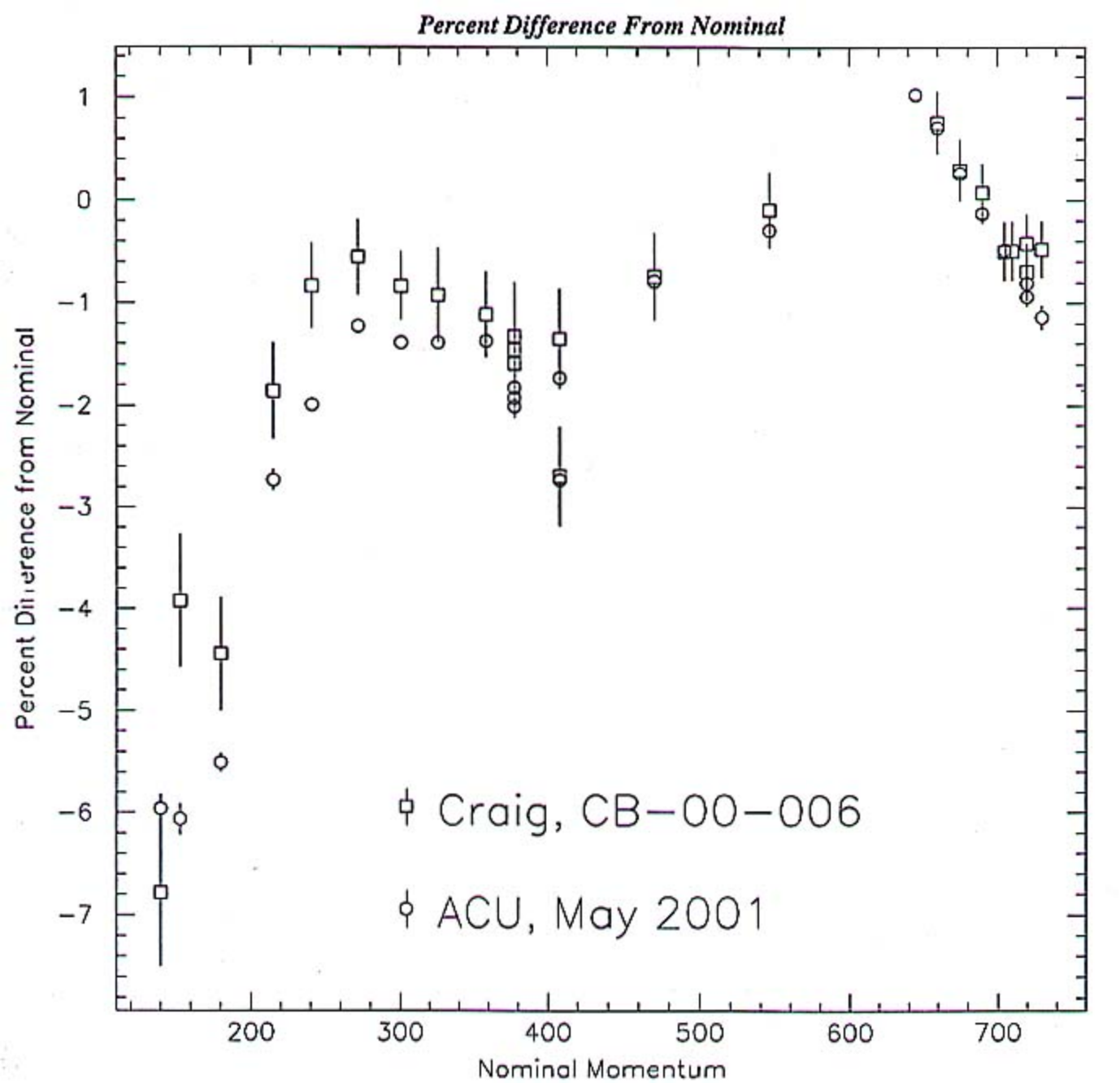
Percent Difference From Nominal
Percent Difference from Nominal
1
0
−1
−2
−3
−4
−5
−6
−7
200
300
400
500
600
700
Nominal Momentum
Craig, CB−00−006
ACU, May 2001

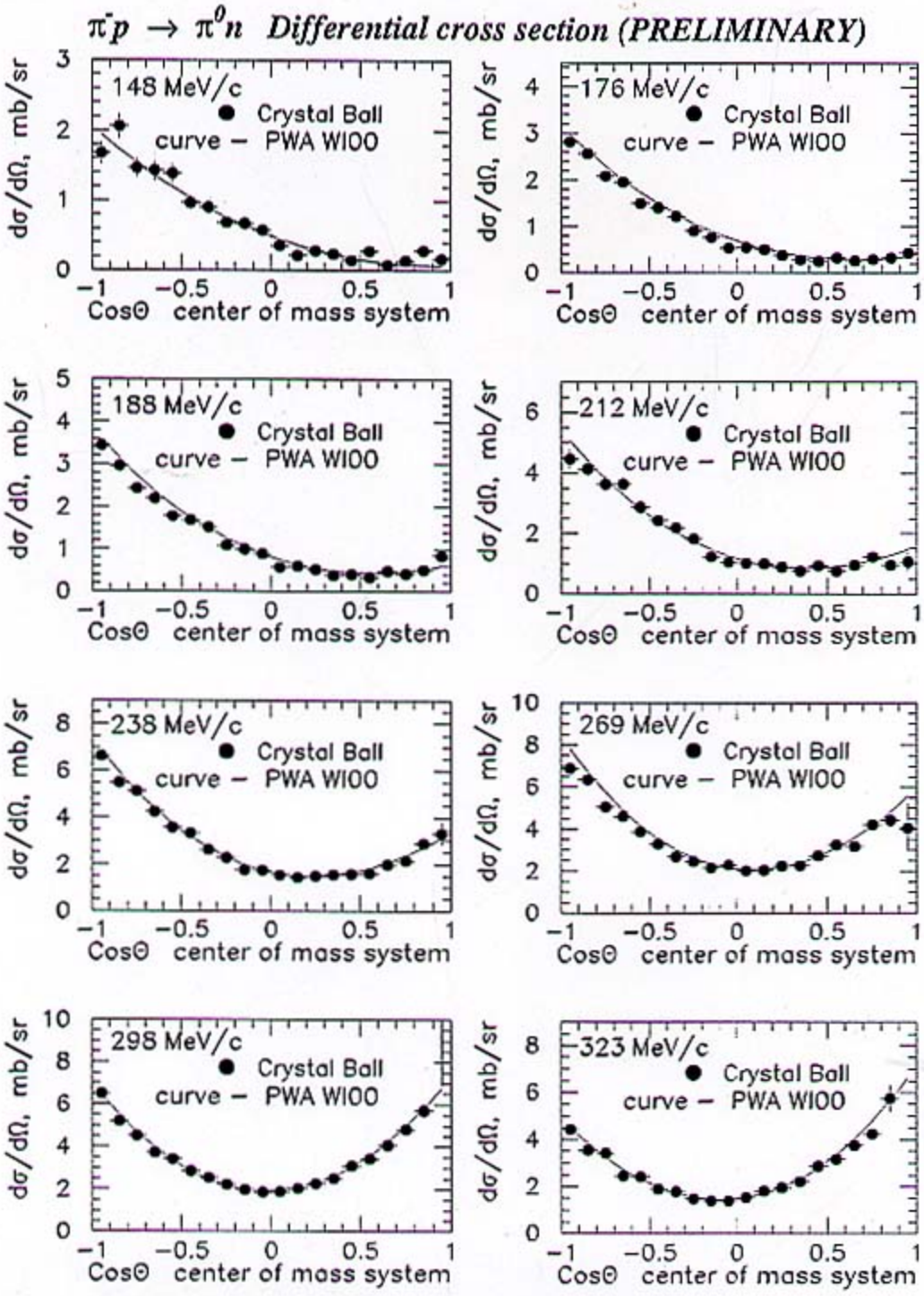

FIGURE 2. Differential cross sections of reaction $\pi^- p \rightarrow \pi^0 n$. Black circles are the preliminary values obtained in this experiment. The curve shows the results of the WI00 partial-wave analysis of the George Washington group [3].

2001/09/24 15.18

$\pi^- p \rightarrow \pi^0 n$ *Differential cross section*

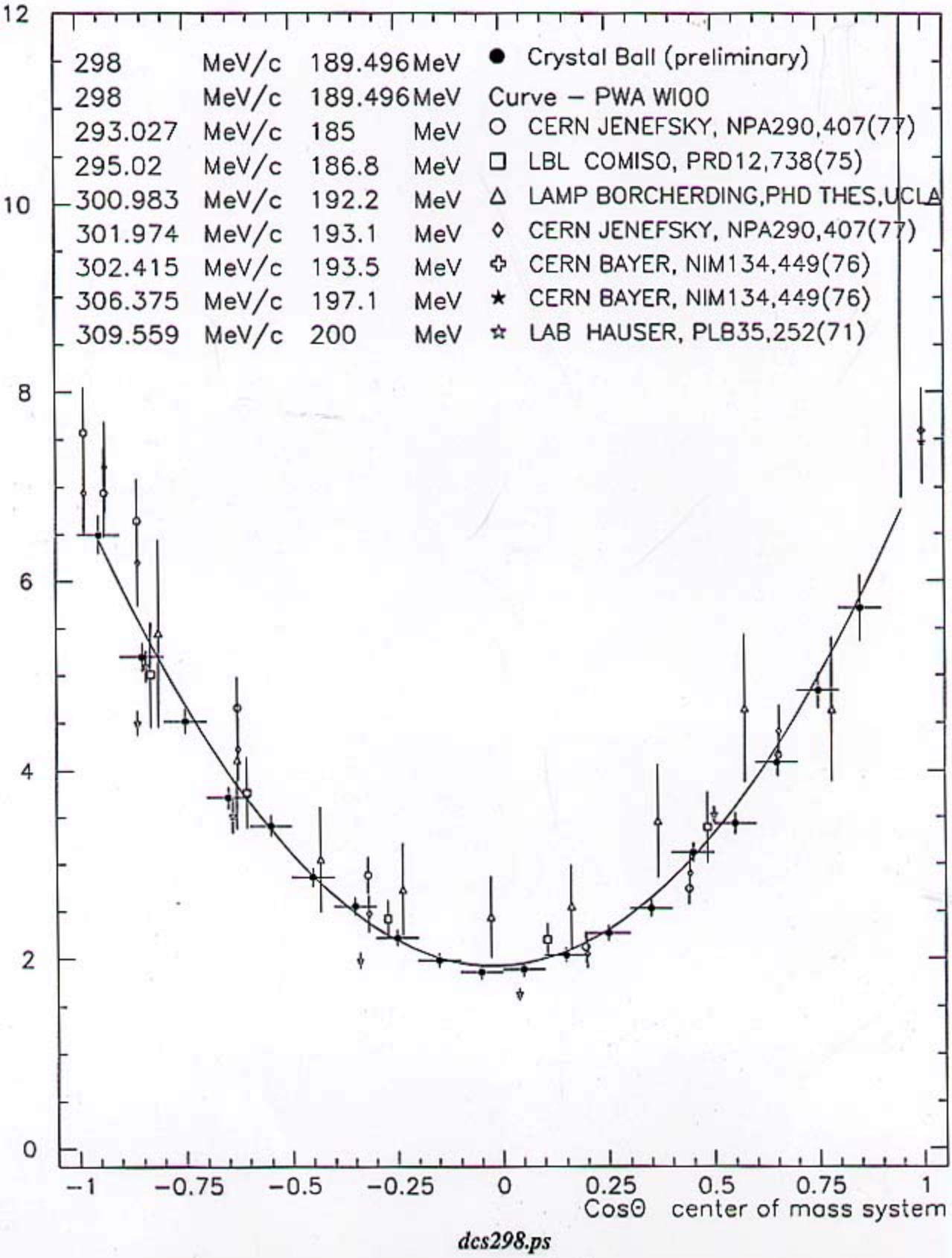

dcs298.ps

$\pi^- p \to \pi^0 n$ (CEX)

2001/07/23 10.41

296.5 MeV/c Differential Cross Section - with Near-Edge Cut

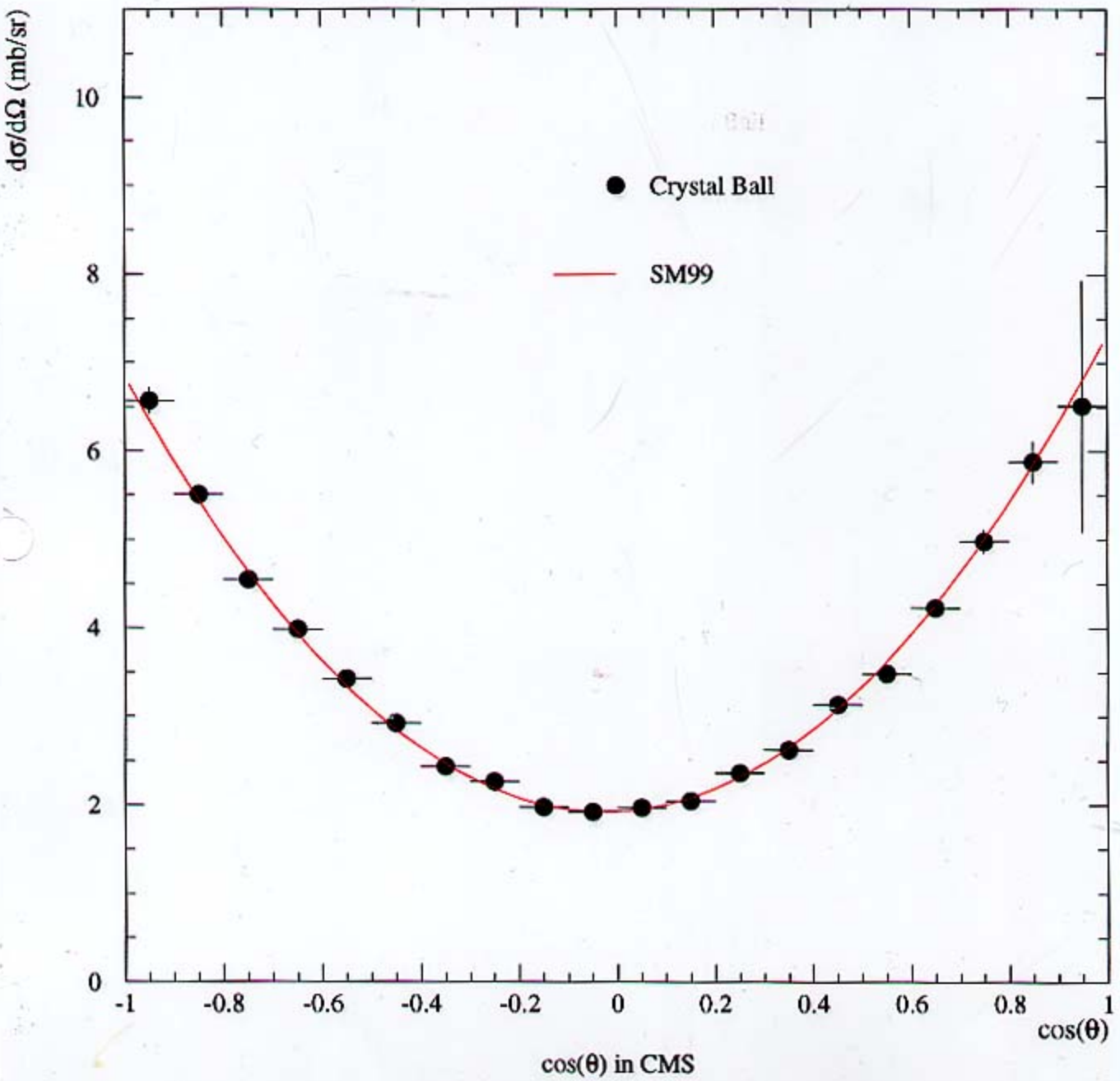

M. Sadler
Crystal Ball

97/10/28 13.09

Exp 913

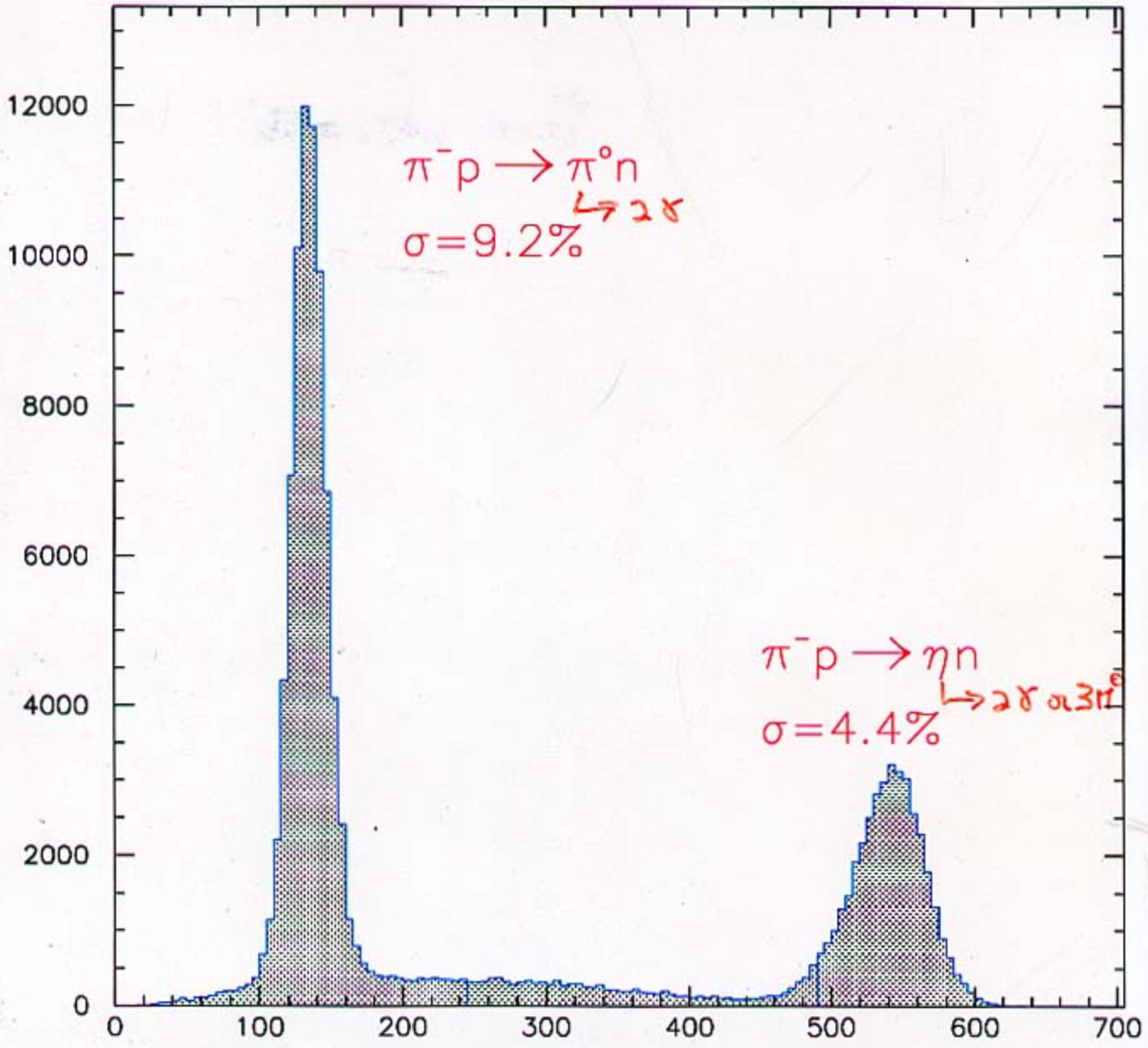

$IM_{\gamma\gamma}$ *for* $800 < MM(MeV/c^2) < 1200$

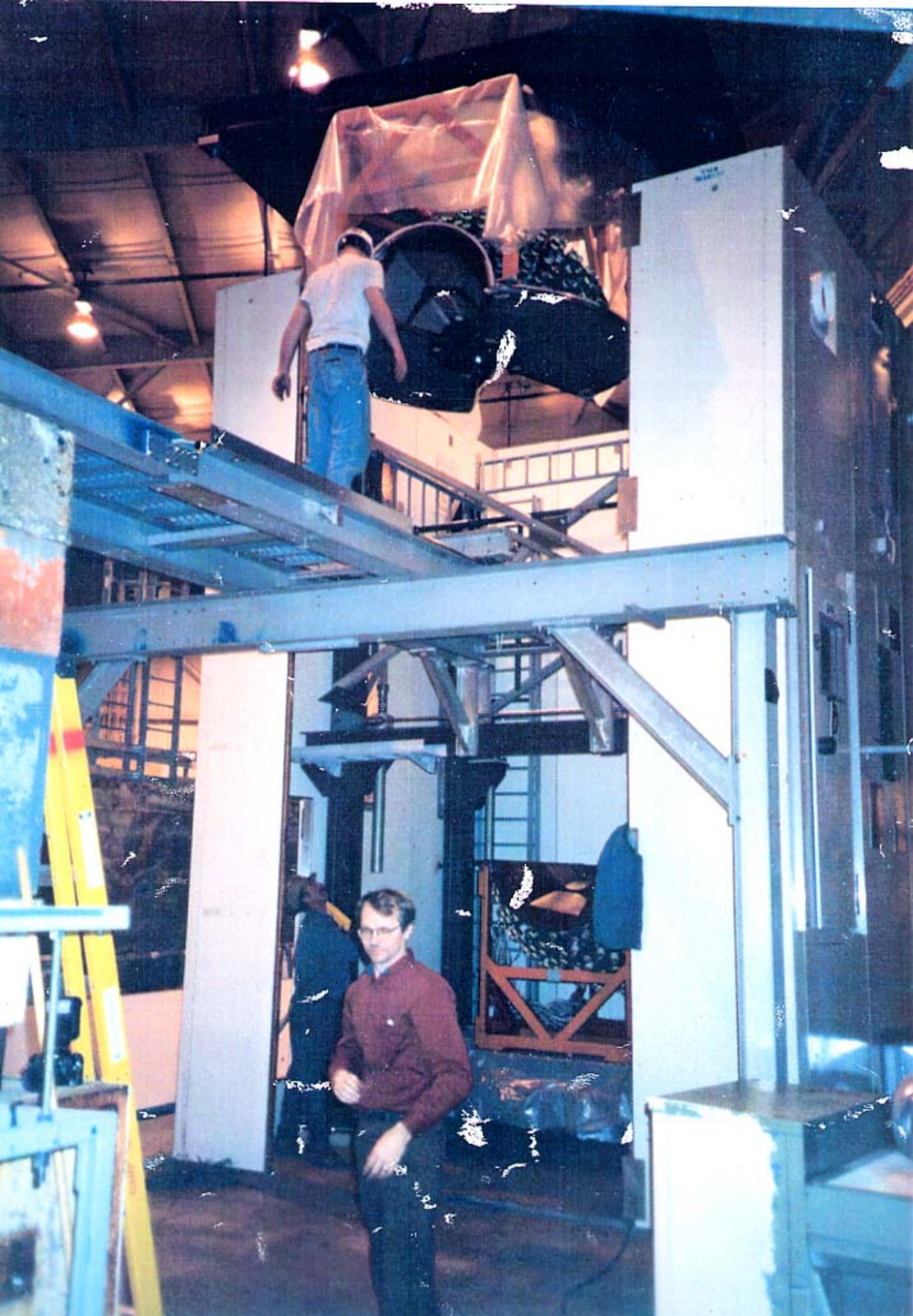

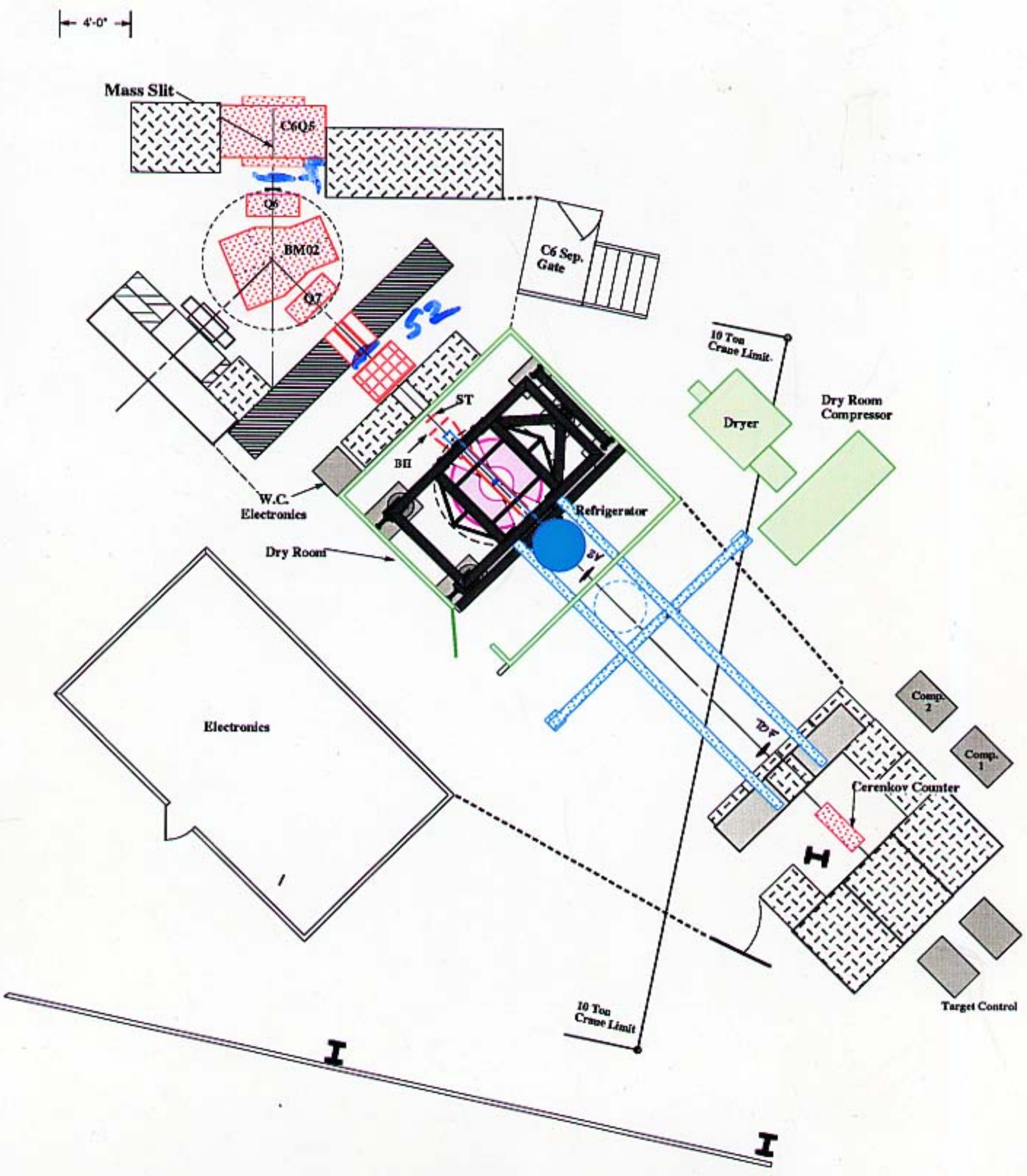
4'-0"
Mass Slit
C6Q5
Q6
BM02
Q7
C6 Sep. Gate
52
10 Ton Crane Limit.
Dryer
Dry Room Compressor
ST
BH
W.C. Electronics
Refrigerator
Dry Room
BV
Electronics
DF
Comp. 2
Comp. 1
Cerenkov Counter
H
Target Control
10 Ton Crane Limit
I
I

Introduction

- Precise data on $\pi^- p$ and $K^- p$ interactions to various neutral final states were measured in 1998 with the Crystal Ball multi-photon spectrometer.
- The measurements were carried out for beam momenta up to $\sim$760 MeV/c at the C6 beam line of the BNL AGS.

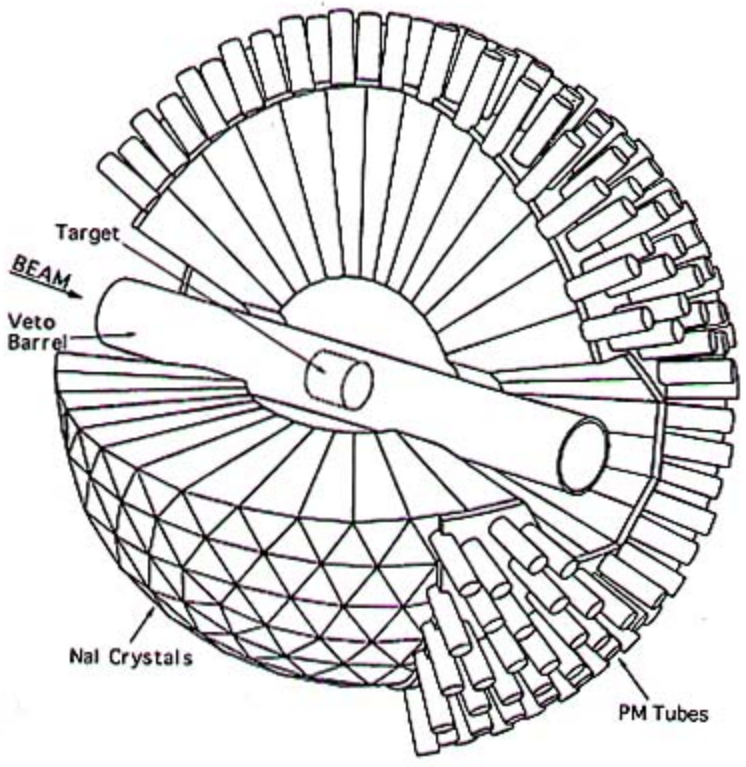

Figure 1: The Crystal Ball multi-photon spectrometer.

1998 Crystal Ball Data

Non-strange Spectroscopy:

$\pi^- p \rightarrow \pi^0 n$
$\pi^- p \rightarrow \pi^0\pi^0 n$
$\pi^- p \rightarrow \pi^0\pi^0\pi^0 n$
$\pi^- p \rightarrow \eta n$
$\pi^- p \rightarrow \gamma n$
$\pi^- p \rightarrow \pi^0\gamma n$
Neutron detection

Nuclear Physics:

$\pi^- A \rightarrow \pi^0 X$
$\pi^- A \rightarrow \pi^0\pi^0 X$
$\pi^- A \rightarrow \eta X$

Eta decays:

$\eta \rightarrow \pi^0\gamma\gamma$
$\eta \rightarrow \pi^0\pi^0\pi^0$
$\eta \rightarrow \pi^0\pi^0$
$\eta \rightarrow \pi^0\pi^0\pi^0\pi^0$
$\eta \rightarrow \pi^0\pi^0\gamma$
$\eta \rightarrow \pi^0\pi^0\pi^0\gamma$
$\eta \rightarrow \gamma\gamma\gamma$

Antiprotons:

$\bar{p}p \rightarrow$ neutrals (π^0, η, ω)

Strange Spectroscopy:

$K^- p \rightarrow \overline{K^0} n$
$K^- p \rightarrow \pi^0 \Lambda$
$K^- p \rightarrow \pi^0\pi^0 \Lambda$
$K^- p \rightarrow \pi^0\pi^0\pi^0 \Lambda$
$K^- p \rightarrow \pi^0 \Sigma$
$K^- p \rightarrow \pi^0\pi^0 \Sigma$
$K^- p \rightarrow \pi^0\pi^0\pi^0 \Sigma$
$K^- p \rightarrow \gamma \Sigma$
$K^- p \rightarrow \gamma \Lambda$
$K^- p \rightarrow \eta \Lambda$

Quantity of data:

20 momenta for $\pi^- p$ { 650 - 760 MeV/c, $\sqrt{s}$ = 1130 - 1530 MeV
2 " $\pi^- A$
1 " $\bar{p}p$
8 " $K^- p$ 500 - 750 MeV/c, $\sqrt{s}$ = 1560 - 1675 MeV
> $2 \cdot 10^7$ η's

CBC Baryon Program

π^- p $\rightarrow$ n γ
n π^0 $\rightarrow$ n 2γ
n η $\rightarrow$ n 2γ
n π^0 π^0 $\rightarrow$ n 4γ
etc.

K^- p $\rightarrow$ Λ γ $\rightarrow$ n π^0 γ $\rightarrow$ n 3γ
Λ π^0 $\rightarrow$ n π^0 π^0 $\rightarrow$ n 4γ
Λ η $\rightarrow$ n π^0 η $\rightarrow$ n 4γ
Λ π^0 π^0 $\rightarrow$ n $3\pi^0$ $\rightarrow$ n 6γ
etc.

Σ^0 γ $\rightarrow$ Λ γ γ $\rightarrow$ n 4γ
etc.

Goal–

Obtain thorough knowledge of baryon spectrum for neutral (photon) final states.

DOUBLE NEUTRAL-PION PRODUCTION IN PION-PROTON INTERACTIONS

by

Kathleen Kelly Craig

A Dissertation Presented in Partial Fulfillment
of the Requirements for the Degree
Doctor of Philosophy

ARIZONA STATE UNIVERSITY

December 2001

Properties of the N(1440) $\frac{1}{2}^+$

Mass	1430-1470 MeV
Width	250-450 MeV
Pole Position	
Re	1345-1385 MeV
Im	160-260 MeV

Decay Modes

$N\pi$	60-70%
$N\eta$	-------
$N\pi\pi$	30-40%
$\Delta\pi$	20-30%
$N\rho$	<8%
$N(\pi\pi)^{I=0}_{s-wave}$	5-10%
$p\gamma$	0.035-0.048%
$n\gamma$	0.009-0.032%

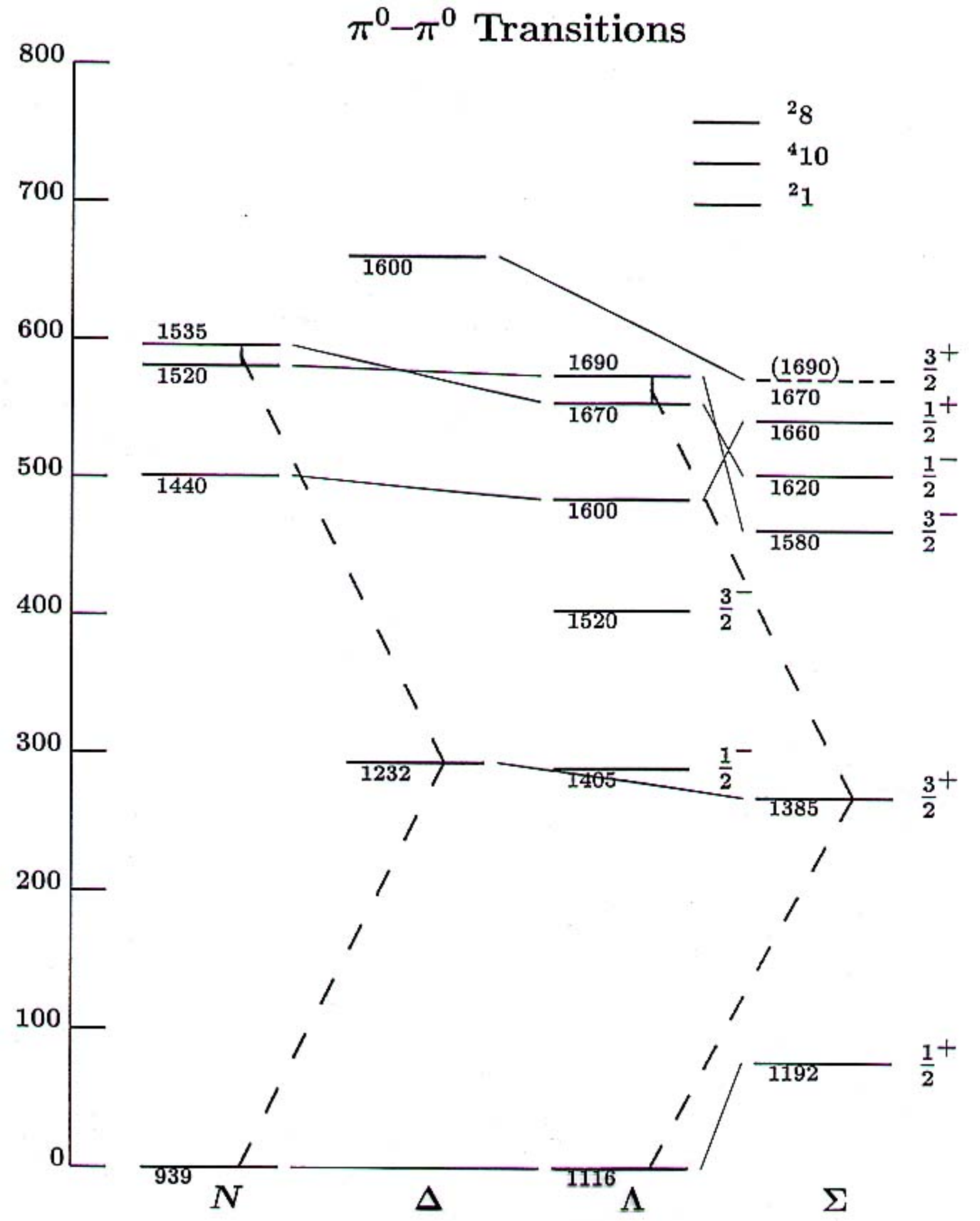
π^0–π^0 Transitions
800
700
600
500
400
300
200
100
0
^{2}8
^{4}10
^{2}1
1600
1535
1520
1690
1670
(1690)
1670
1660
1440
1600
1620
1580
1520
$\frac{3}{2}^-$
1232
1405
$\frac{1}{2}^-$
1385
$\frac{3}{2}^+$
$\frac{3}{2}^+$
$\frac{1}{2}^+$
$\frac{1}{2}^-$
$\frac{3}{2}^-$
1192
$\frac{1}{2}^+$
939
1116
N
Δ
Λ
Σ

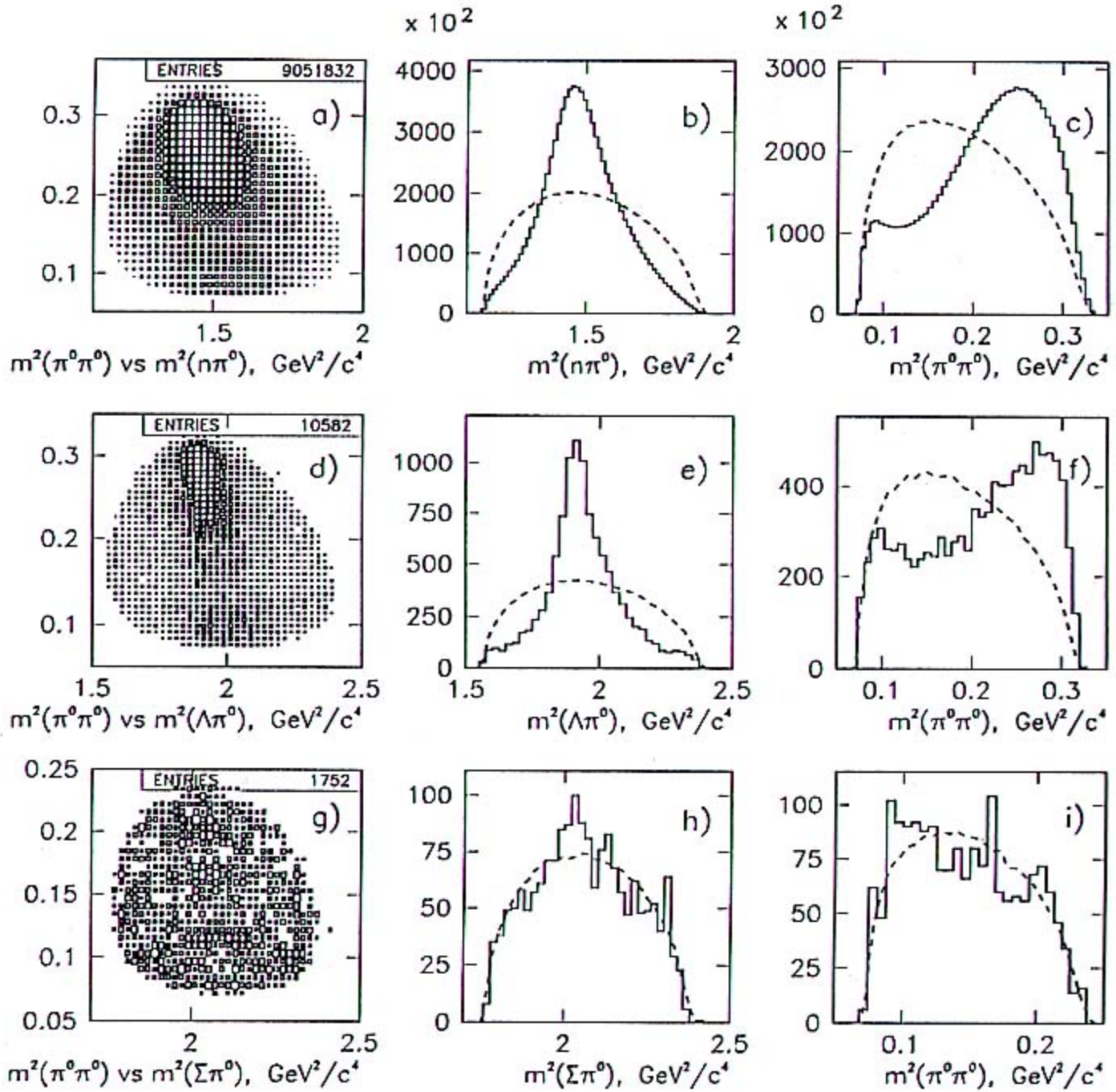

Figure 5. Figures a–c: $\pi^- p \to \pi^0\pi^0 n$ at $p_{\pi^-} = 720$ MeV/c; d–f: $K^- p \to \pi^0\pi^0\Lambda$ at $p_{K^-} = 750$ MeV/c; g–i: $K^- p \to \pi^0\pi^0\Sigma^0$ at $p_{K^-} = 750$ MeV/c. Preliminary data. The dashed lines show the phase space.

Data

$K^- p \to \pi^0 \pi^0 \Lambda$

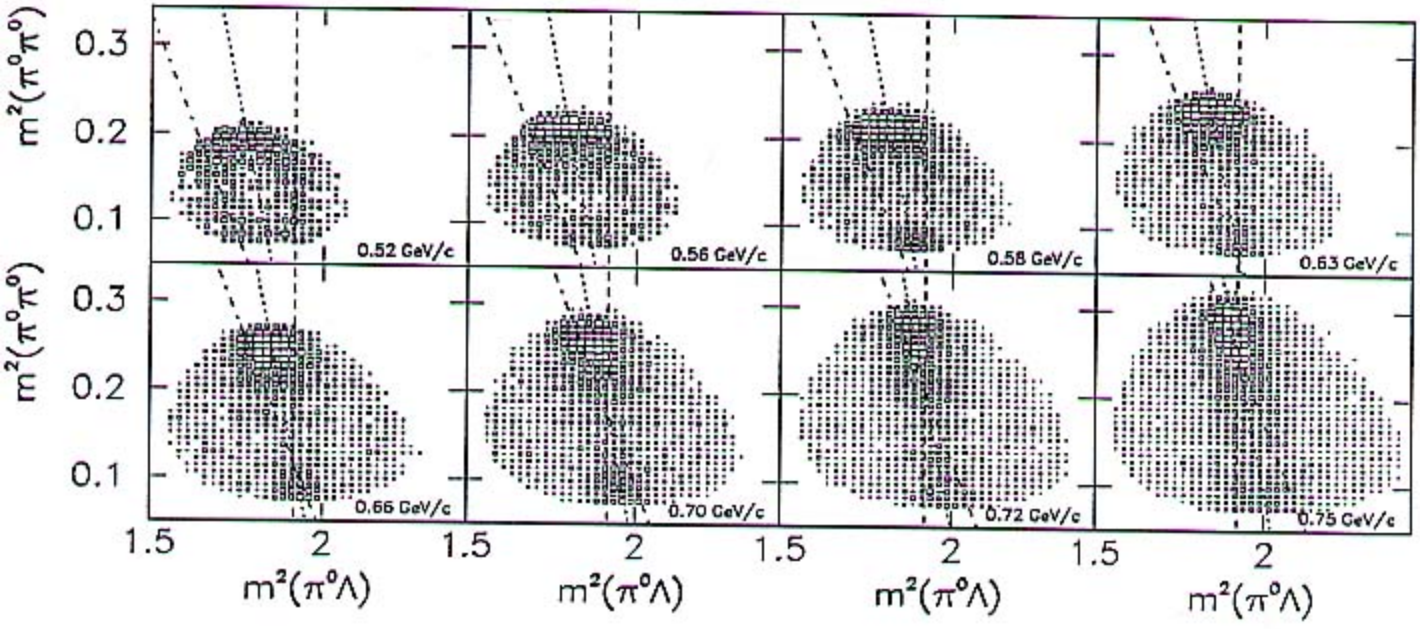

Dashed lines are predictions for

$m^2(\pi^0 \Lambda) = m^2(\Sigma^*)$ with $m(\Sigma^*) = 1.385$ GeV

Data

$\pi^- p \to \pi^0 \pi^0 n$

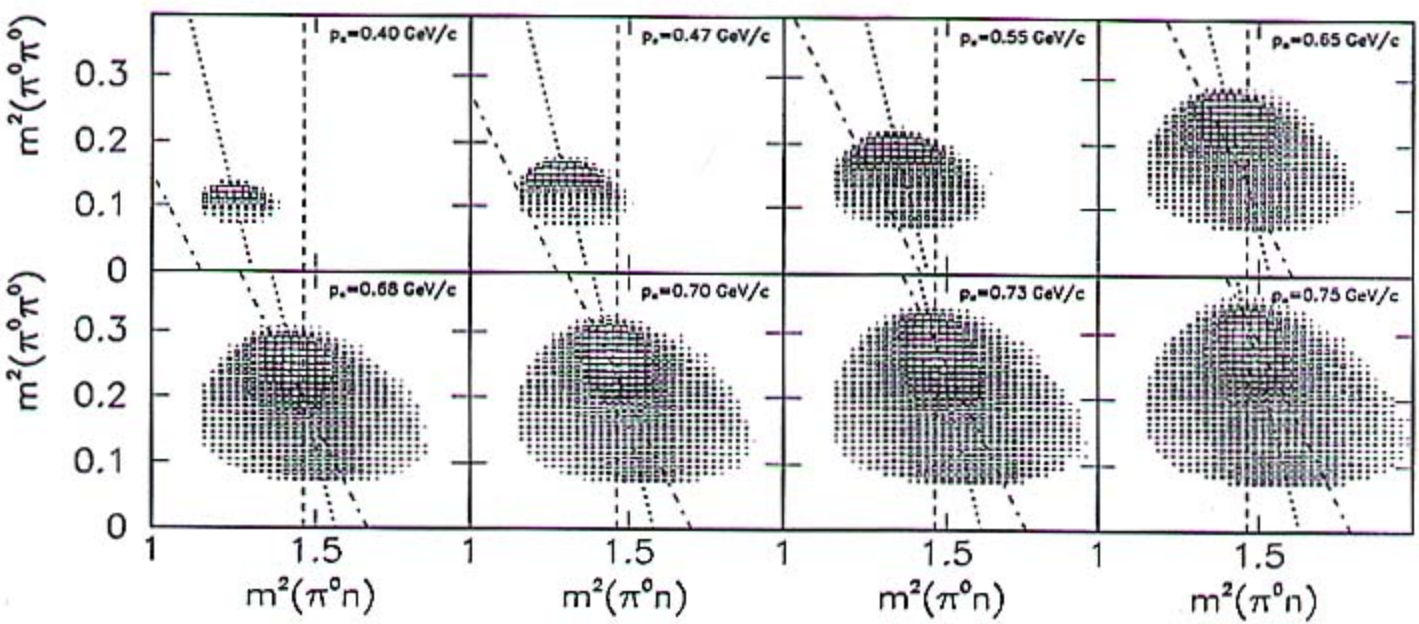

$\pi^- p \to \pi_1^0 \Delta^0$

$\hookrightarrow \pi_2^0 n$

Monte Carlo

$p_{\pi^-} = 0.73$ GeV/c

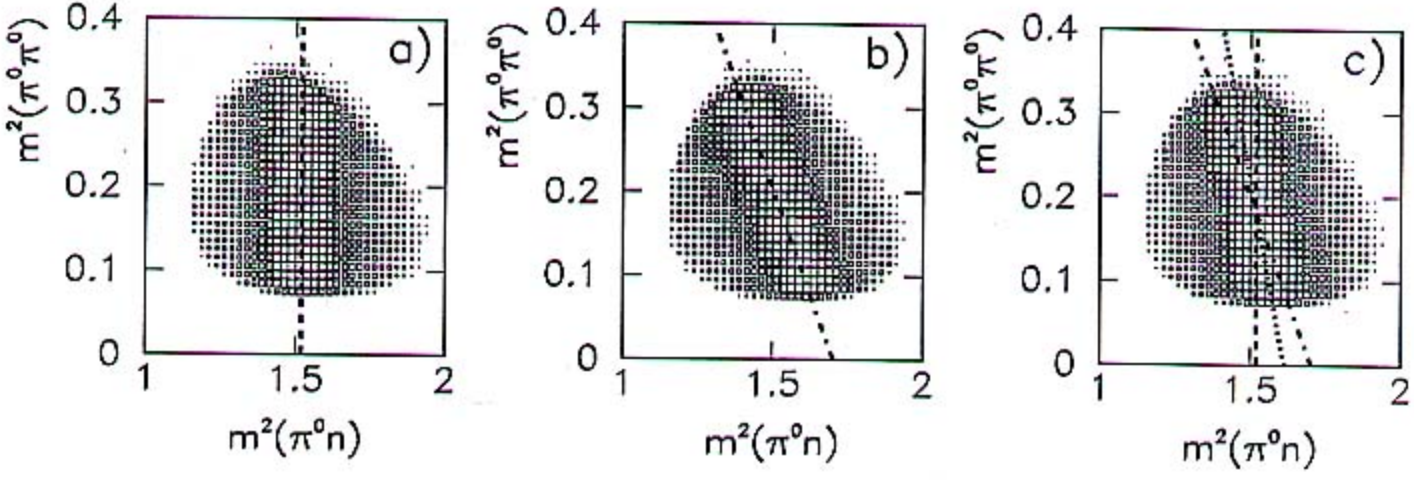

$m(\pi_2^0 n)$ $m(\pi_1^0 n)$ Sum

Monte Carlo

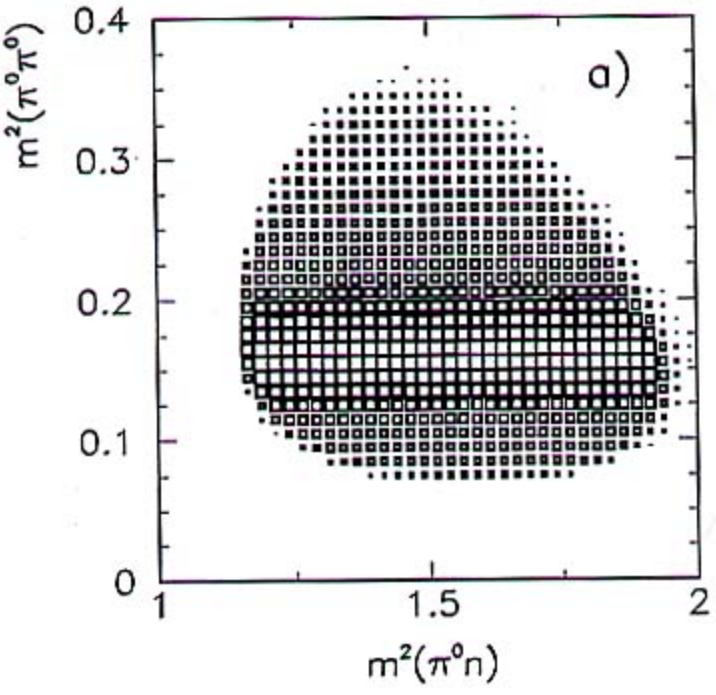

$\pi^- p \to f_0 n$

$\hookrightarrow \pi^0\pi^0$

Assumptions:

$m(f_0) = 0.4$ GeV

$\Gamma(f_0) = 0.1$ GeV

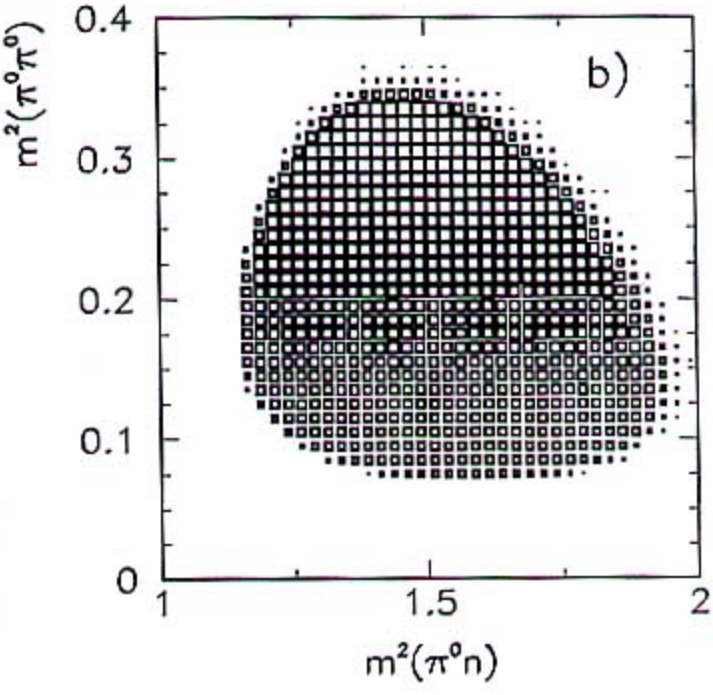

$\pi^- p \to f_0 n$

$\hookrightarrow \pi^0\pi^0$

Assumptions:

$m(f_0) = 0.75$ GeV

$\Gamma(f_0) = 0.40$ GeV

Mechanisms for $\pi^- p \rightarrow \pi^0\pi^0 n$

Pion Exchange

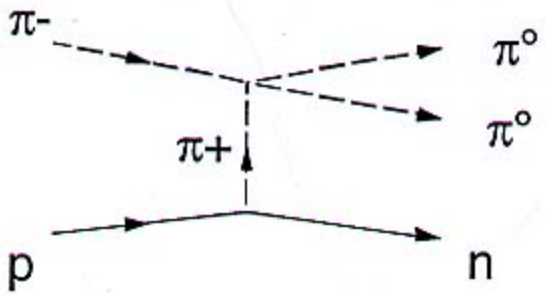

N* Production, f_0 (or "σ") Decay

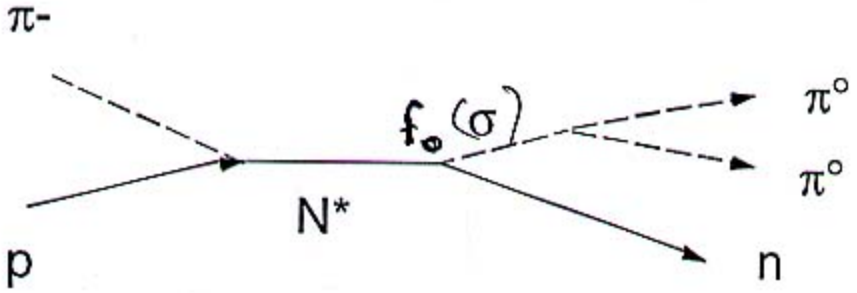

N* Production, Sequential Decay

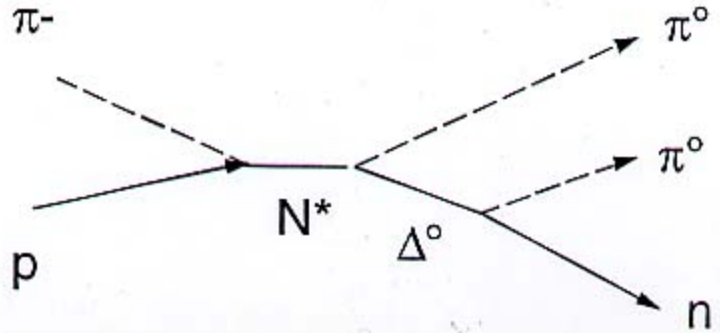

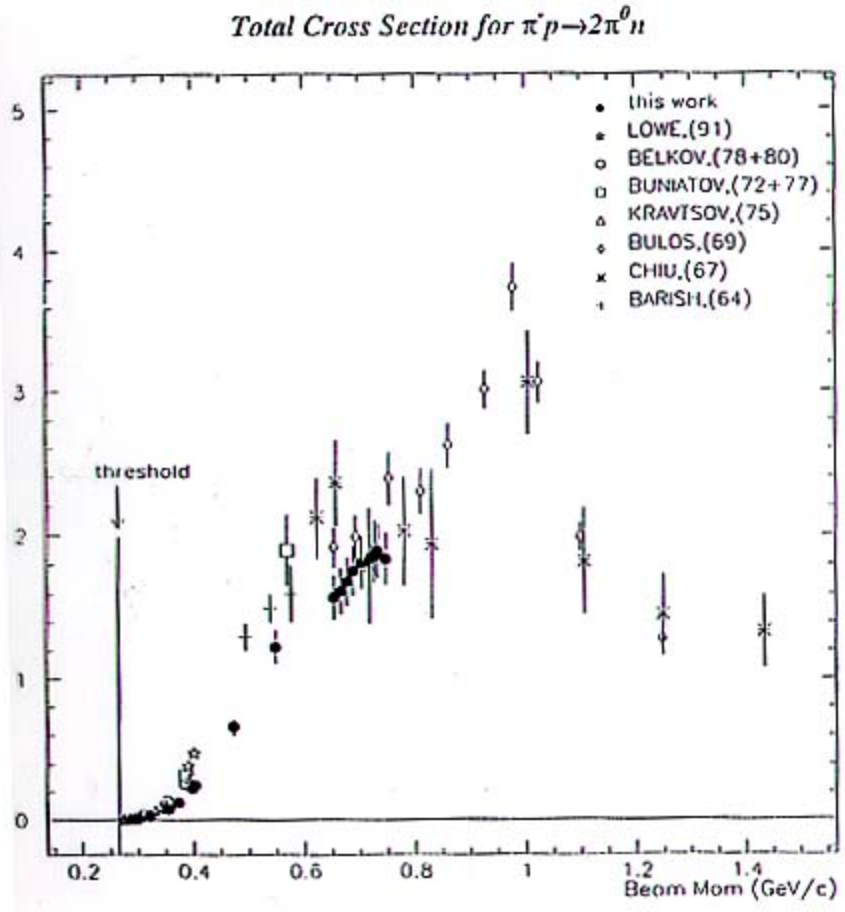
Total Cross Section for $\pi^- p \to 2\pi^0 n$
this work
LOWE.(91)
BELKOV.(78+80)
BUNIATOV.(72+77)
KRAVTSOV.(75)
BULOS.(69)
CHIU.(67)
BARISH.(64)
threshold
Beam Mom (GeV/c)

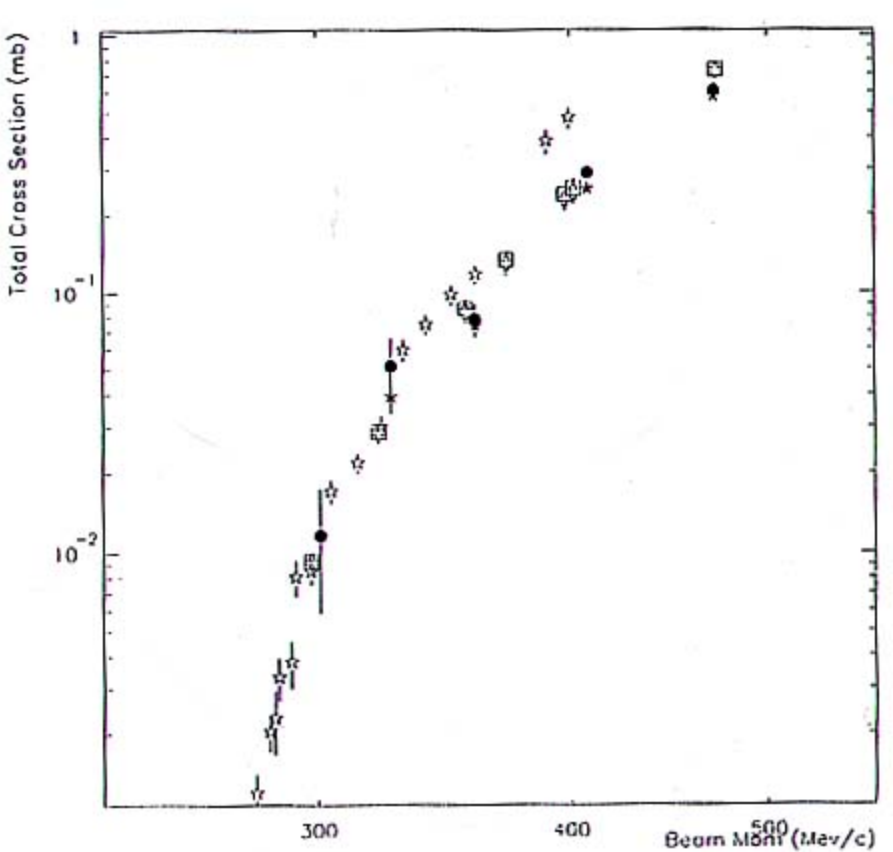
Total Cross Section (mb)
Beam Mom (Mev/c)

$K^- p$ Selectivity

$K^- p \to \eta\Lambda$

$K^- p \to \pi^0\Sigma^0$

} Pure $I = 0$ Selects Λ^*

$K^- p \to \pi^0\Lambda$ Pure $I = 1$ Selects Σ^*

$K^- p \to \overline{K^0} n$ Mixed $I = 0,\ 1$

UNIVERSITY OF CALIFORNIA

Los Angeles

First Measurement of the Radiative Process $K^-p \to \Lambda\gamma$ at Beam Momenta 520 – 750 MeV/c Using the Crystal Ball Detector

A dissertation submitted in partial satisfaction of the

requirements for the degree Doctor of Philosophy

in Physics

by

Nakorn Phaisangittisakul

2001

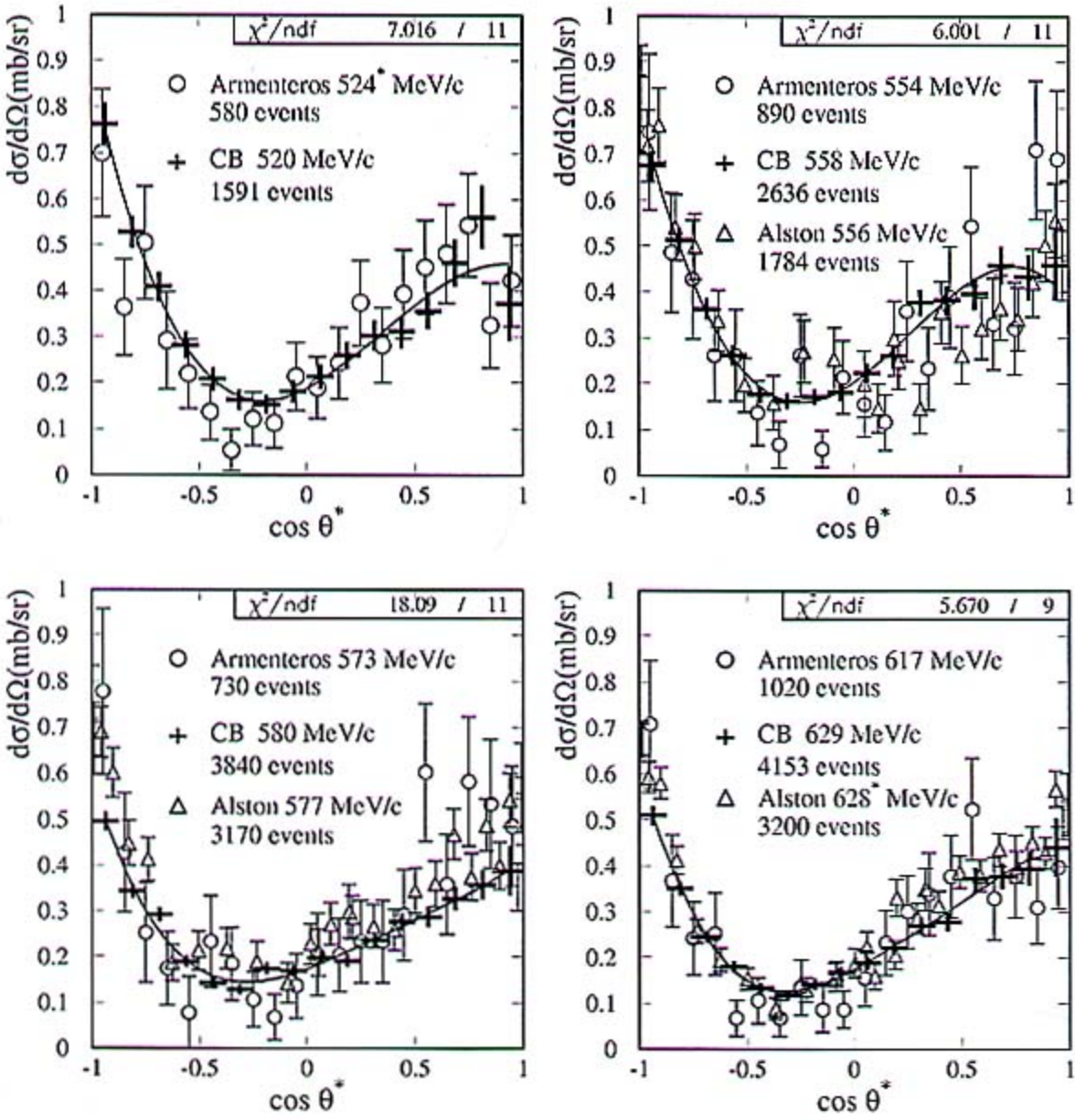

Figure 5.8: Angular distribution of $\bar{K}^0$ in the center-of-mass for the reaction $K^- p \to \bar{K}^0 n$ at $p_K = 520$, 558, 580, and 629 MeV/c. The open circle and triangle are the results from Ref. [44] and Ref. [45] respectively; when the momentum is given with an asterisk, the results for the two nearby momenta have been averaged. The solid curved line is the result of the Legendre polynomial fit to our data.

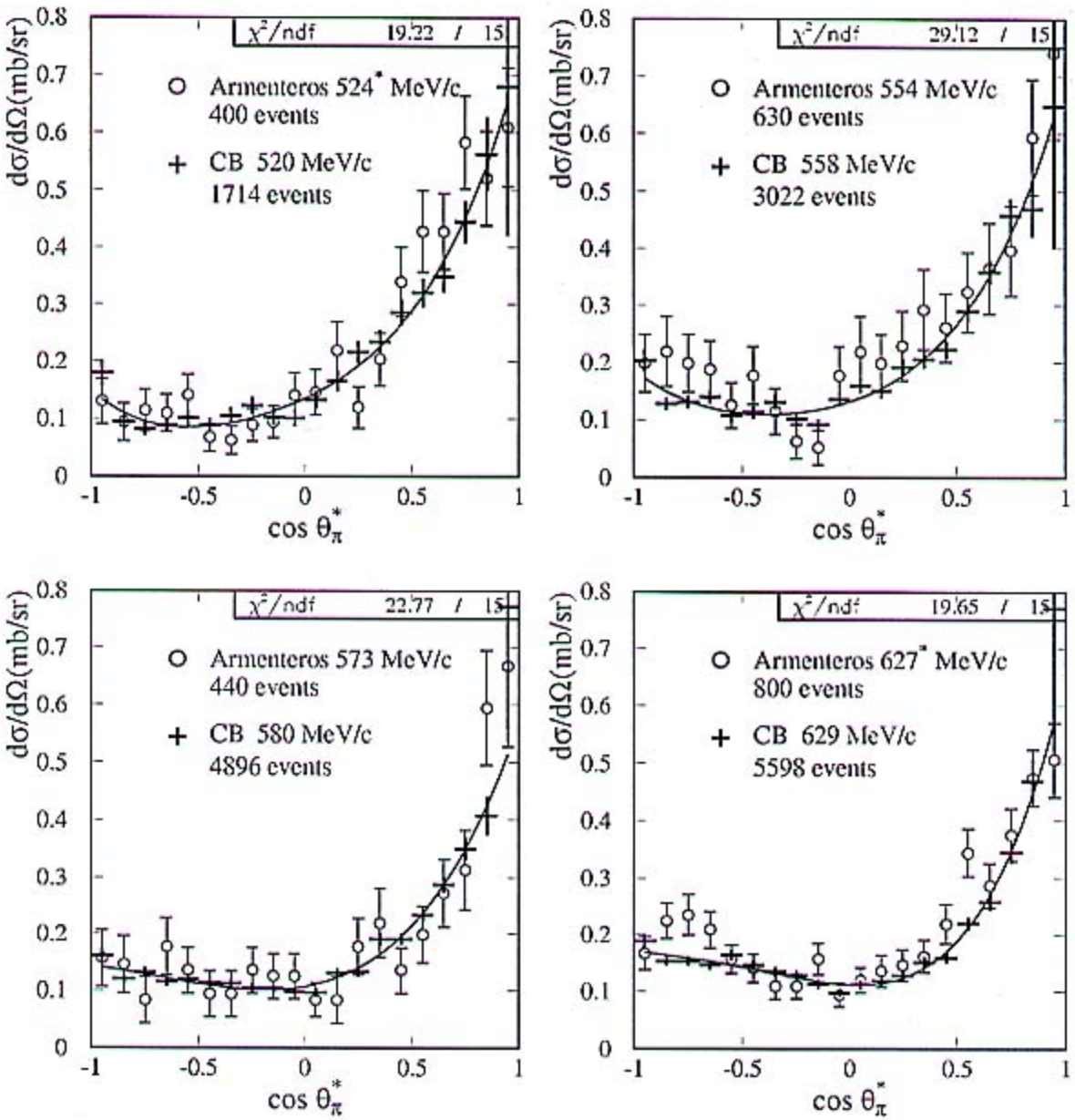

Figure 5.2: Angular distribution of the π^0 in the center-of-mass for the reaction $K^-p \to \Lambda\pi^0$ of the 520, 558, 580, and 629 MeV/c data. Shown by open circles are the results from Ref. [44]; when the momentum has an asterisk, the Armenteros' data from the two nearest momenta have been averaged. The errors in $\frac{d\sigma}{d\Omega}$ are statistical only. The solid curved line is the Legendre polynomial fit to our data.

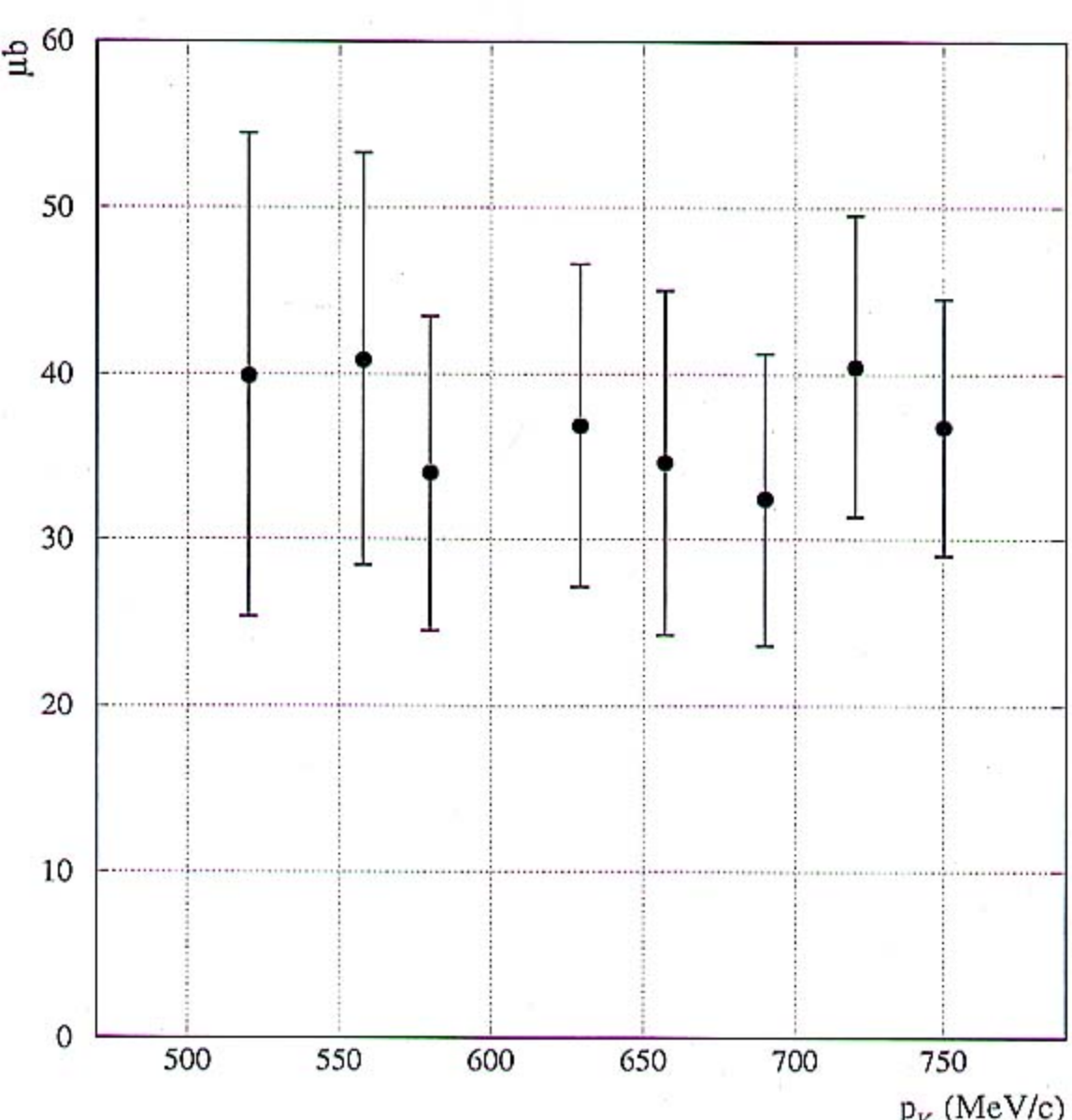

Figure 5.14: $\hat{\sigma}(K^- p \to \Lambda\gamma)$ obtained from the combination of 3- and 4-cluster events at 20% CL.

Experimental Study of the $K^- p \to \pi^0 \Lambda$ Reaction

A dissertation submitted
to Kent State University in partial
fulfillment of the requirements for the
degree of Doctor of Philosophy

by

John A. Olmsted

August, 2001

Threshold η Production

$\pi^- p \to \eta n$ and $K^- p \to \eta \Lambda$ are similar near threshold:

- σ_t rises steeply at opening of η channel.
- s-wave dominance, with similar coefficients –

$$\sigma_t(\pi^- p) = (21 \pm 2)\,(\mu\text{b}/(\text{MeV/c})) \times p^*_\eta$$
$$\sigma_t(K^- p) = (19 \pm 4)\,(\mu\text{b}/(\text{MeV/c})) \times p^*_\eta$$

- Similar maximum total cross sections –

$$\sigma_t(\pi^- p) = 2.6 \pm 0.3 \text{ mb at } p^*_\eta = 182 \text{ MeV/c}$$
$$\sigma_t(K^- p) = 1.5 \pm 0.1 \text{ mb at } p^*_\eta = 81 \text{ MeV/c}$$

- Similar angular distributions, with slight bowl shape (*small* D-wave).

Supports the view that $N(1535)\frac{1}{2}^-$ and $\Lambda(1670)\frac{1}{2}^-$ belong to same $SU(3)$ octet.

$K^- p \to \eta \Lambda$

(Preliminary)

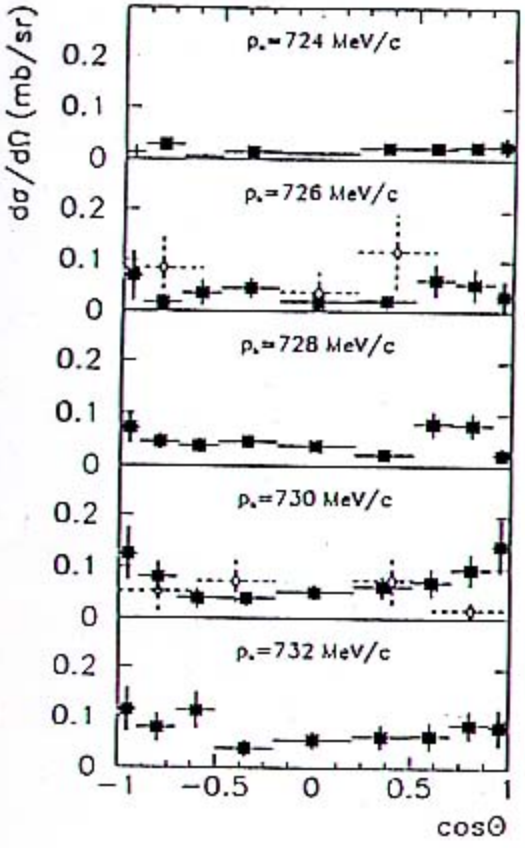

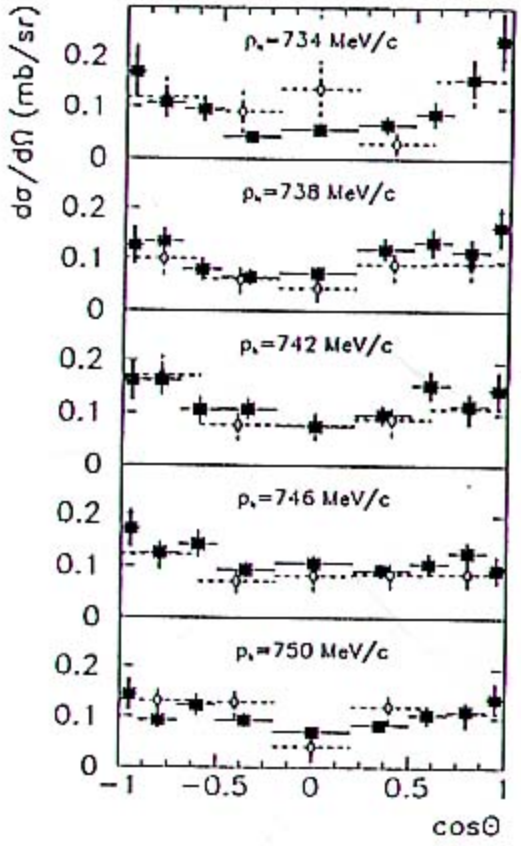

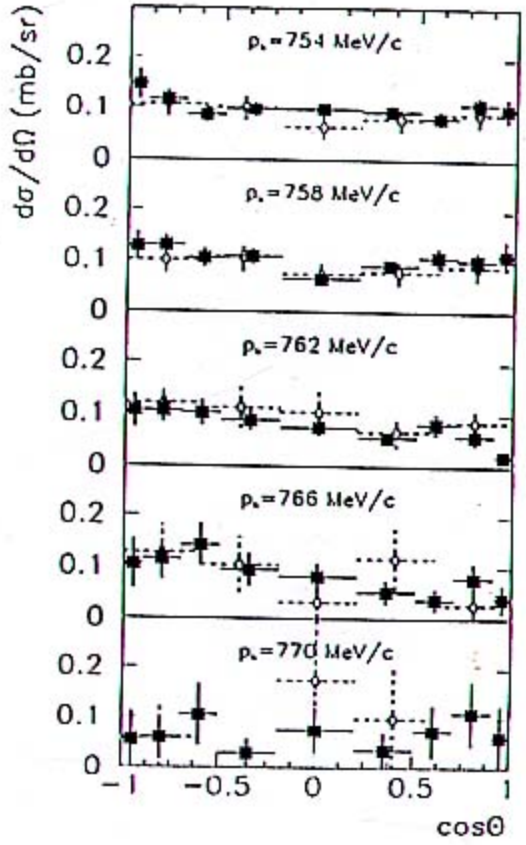

$K^- p \to \eta \Lambda$

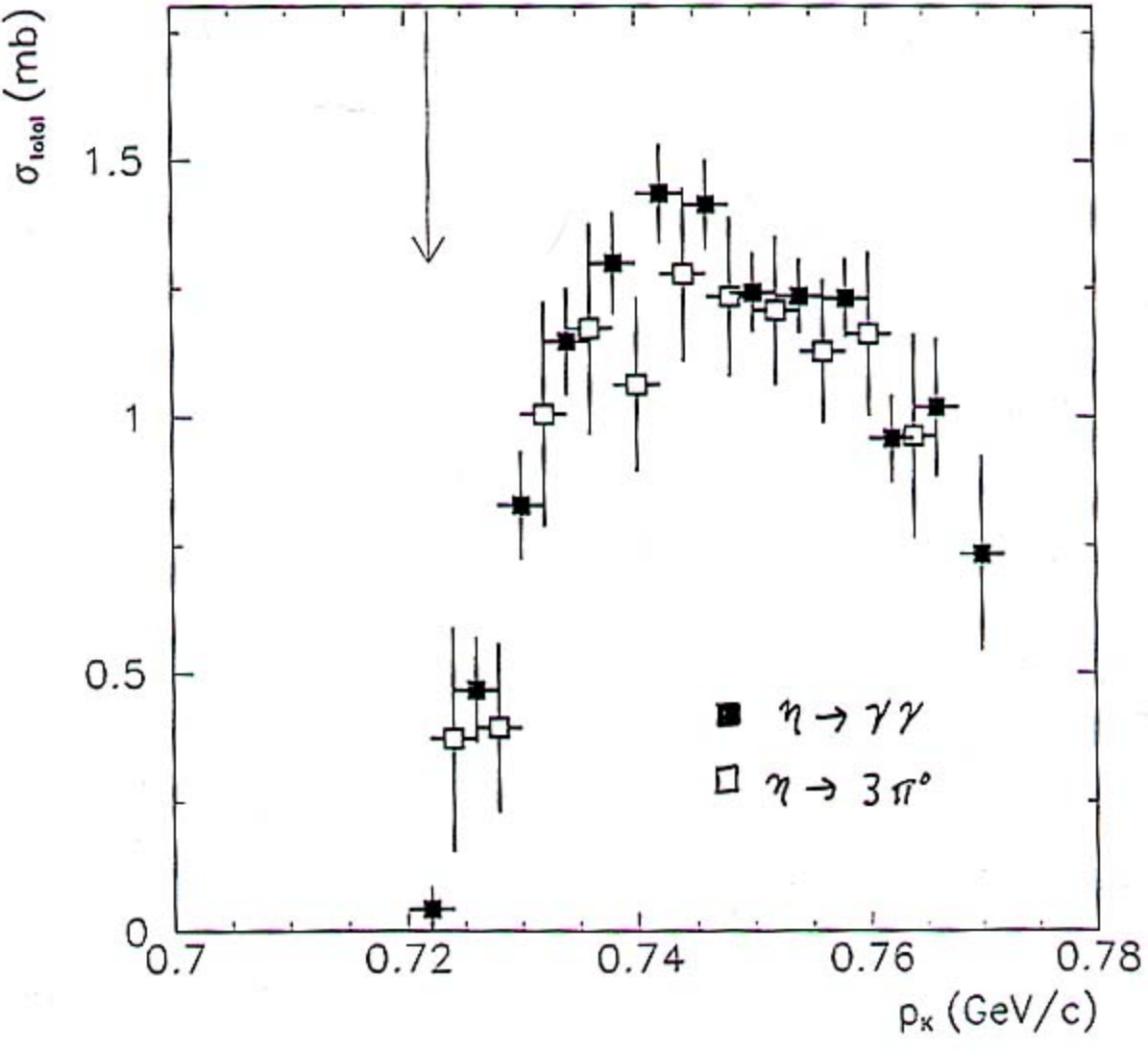

Channel	Γ_i (MeV)	$x_i = \Gamma_i/\Gamma$ (%)	$t = \sqrt{x x_i}$
$\overline{K}N$	8.5 ± 2.6	37.3 ± 6.8	0.37 ± 0.07
$\eta\Lambda$	3.6 ± 1.4	15.7 ± 5.5	0.24 ± 0.04
$\pi\Sigma$	8.8 ± 3.2	38.6 ± 7.9	-0.38 ± 0.03
$\pi\Sigma(1385)$	1.7 ± 1.5	7.6 ± 6.0	-0.17 ± 0.06
$\pi\pi\Lambda$	< 1	< 4	0.05 ± 0.11
$\pi\pi\Sigma$	< 1	< 1	0.00 ± 0.06

Table 2: Resonance parameters for the $\Lambda(1670)$ as determined from our multichannel fit. The fitted Breit-Wigner mass and total width have the values $M = 1673 \pm 2$ MeV and $\Gamma = 23 \pm 6$ MeV, respectively. The corresponding pole position is $(1671 - \mathrm{i}11)$ MeV. In the columns below, Γ_i is the partial width for the i-th decay channel evaluated at the resonance energy, x_i is the corresponding branching fraction, $x = 0.37 \pm 0.07$ is the elasticity, and t is the amplitude at resonance excluding contributions from nonresonant background.

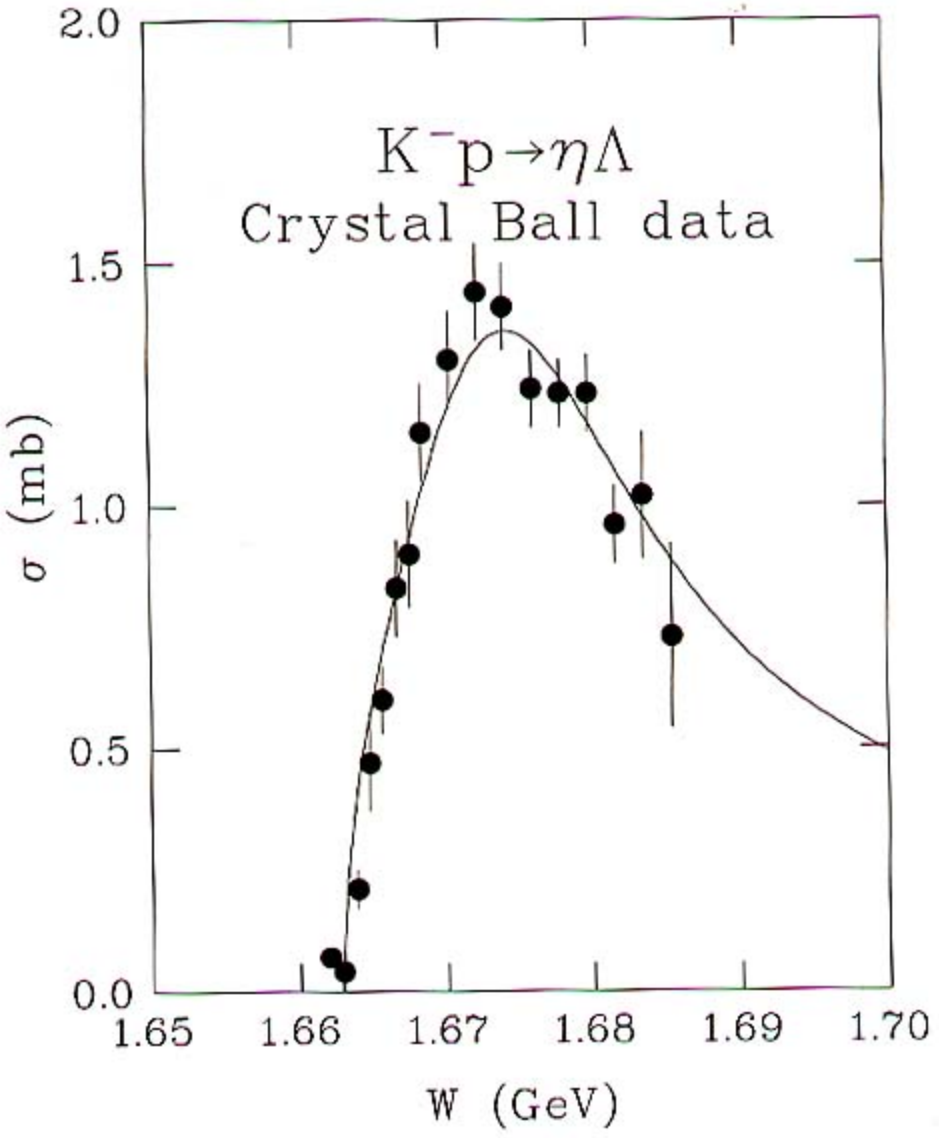

Total cross section for the $K^- p \to \eta\Lambda$ as measured by the Crystal Ball Collaboration. The curve shows the result of a unitary six-channel fit assuming S-wave dominance.

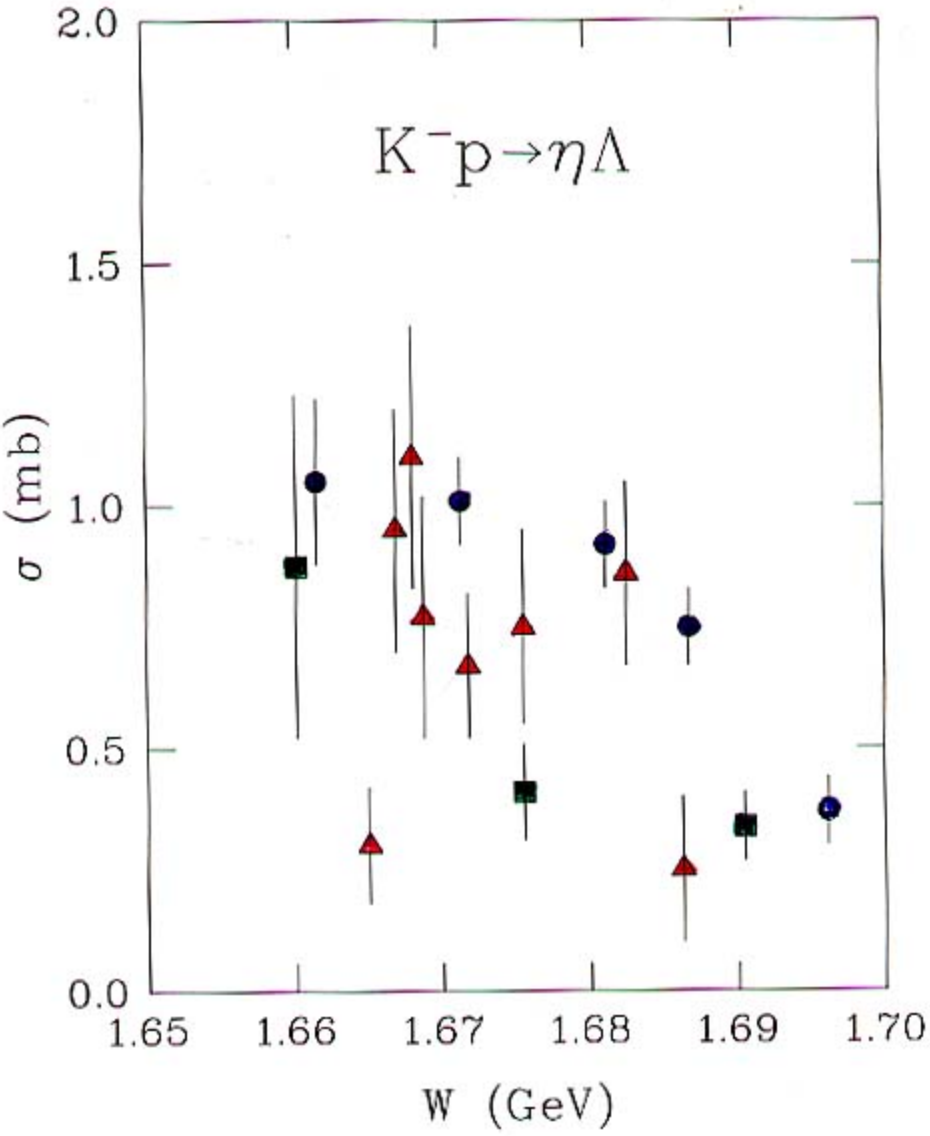

Total cross section for the $K^-p \to \eta\Lambda$ from selected older experiments. Triangles are from D. Berley *et al.*, Phys. Rev. Lett. **15**, 641 (1965); circles are from R. Armenteros *et al.*, Nucl. Phys. **B21**, 15 (1970); and squares are from G. W. London *et al.*, Nucl. Phys. **B85**, 289 (1975).

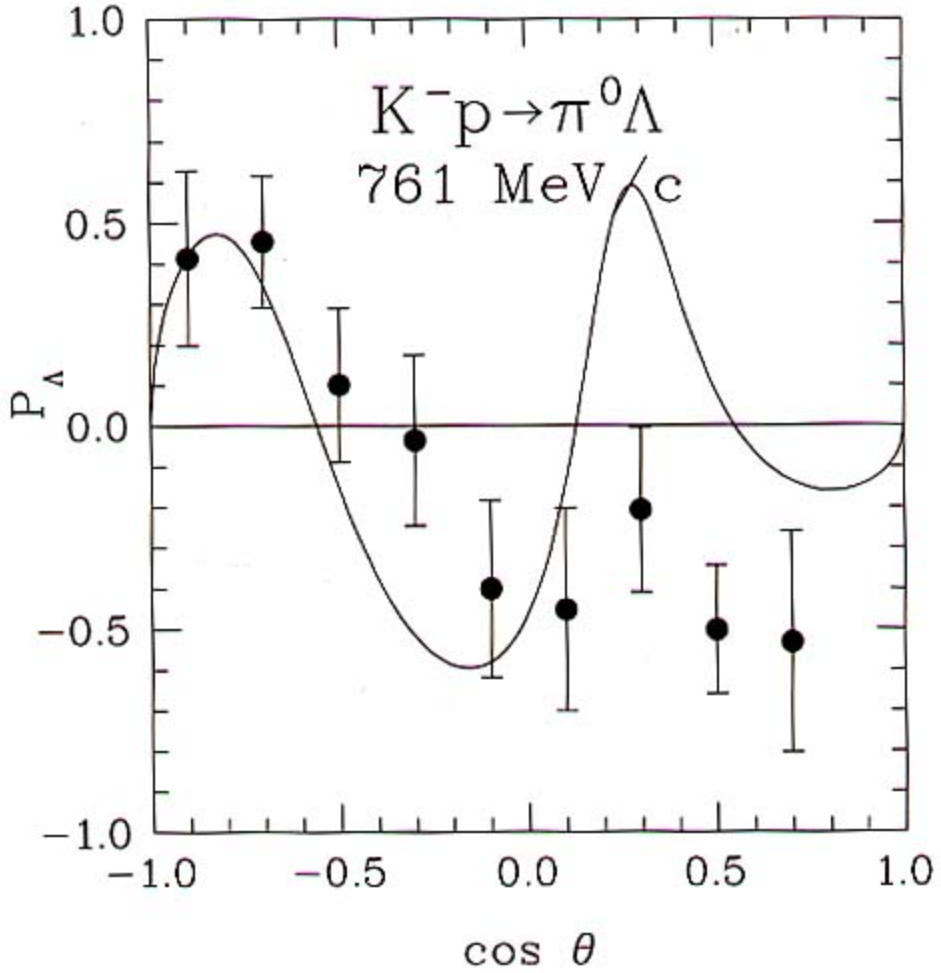

Fig. 7: Preliminary results by Crystal Ball Collaboration for Λ polarization in $K^-p \to \pi^0\Lambda$ at $P_{K^-} = 761$ MeV/c, or $W = 1681$ MeV. The curve is the prediction of the GOPAL 77 partial-wave analysis.

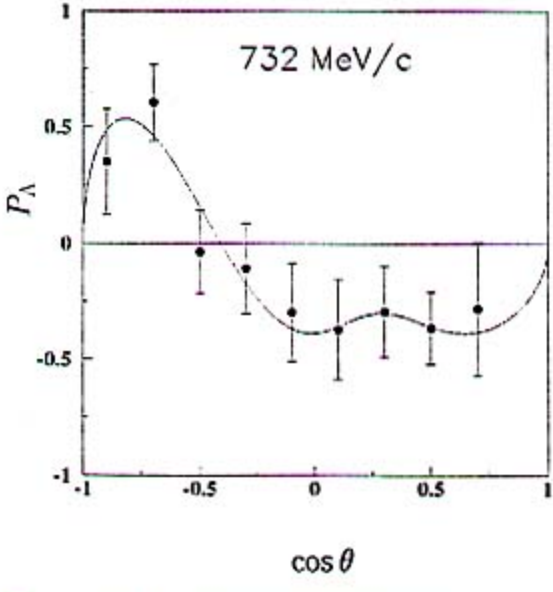

Fig. 4-35: Polarization for the reaction $K^-p \to \pi^0\Lambda$ at 732 MeV/c.

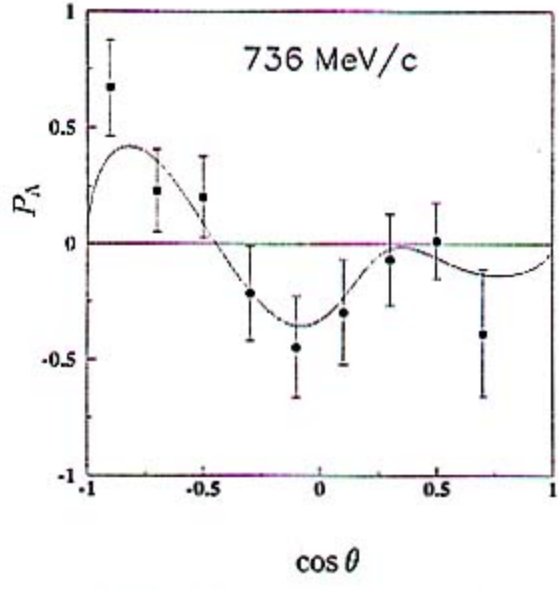

Fig. 4-36: Polarization for the reaction $K^-p \to \pi^0\Lambda$ at 736 MeV/c.

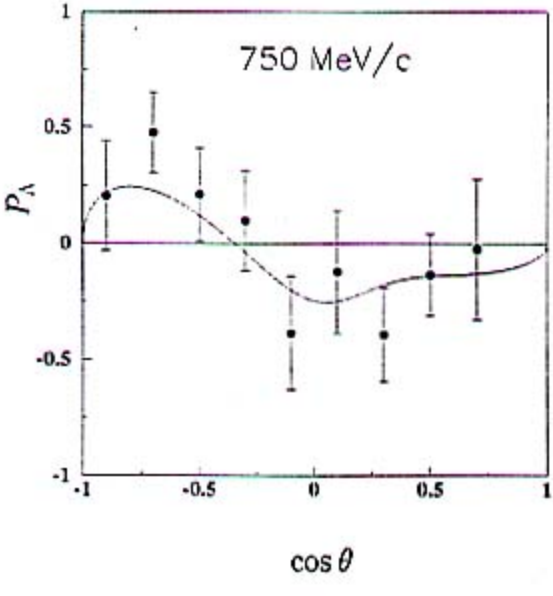

Fig. 4-37: Polarization for the reaction $K^-p \to \pi^0\Lambda$ at 750 MeV/c.

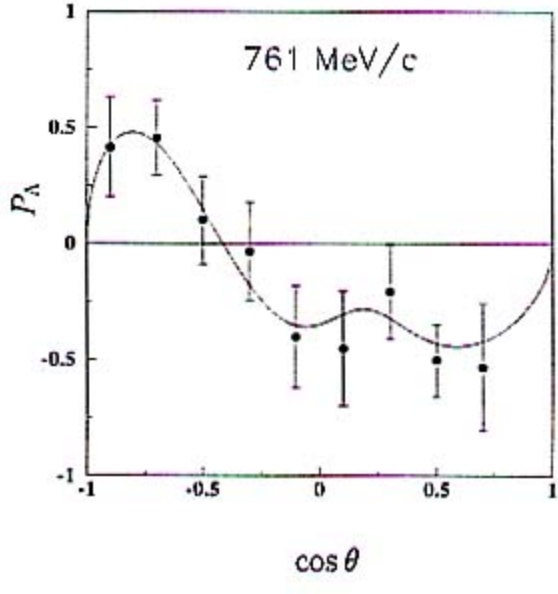

Fig. 4-38: Polarization for the reaction $K^-p \to \pi^0\Lambda$ at 761 MeV/c.

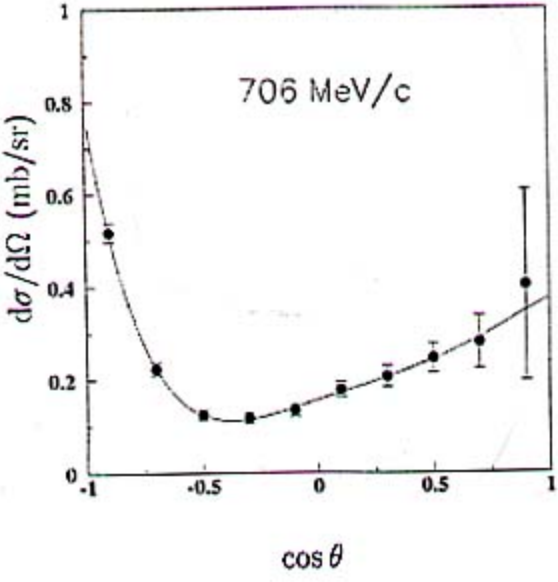

Fig. 4-73: Differential cross section for the reaction $K^-p \to \overline{K^0}n$ at 706 MeV/c.

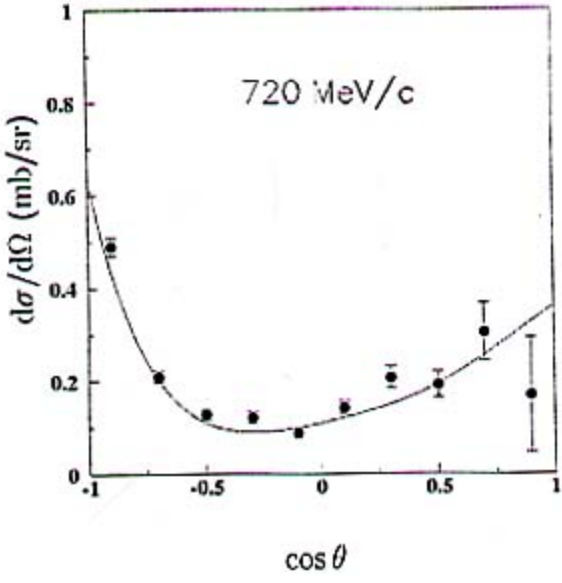

Fig. 4-74: Differential cross section for the reaction $K^-p \to \overline{K^0}n$ at 720 MeV/c.

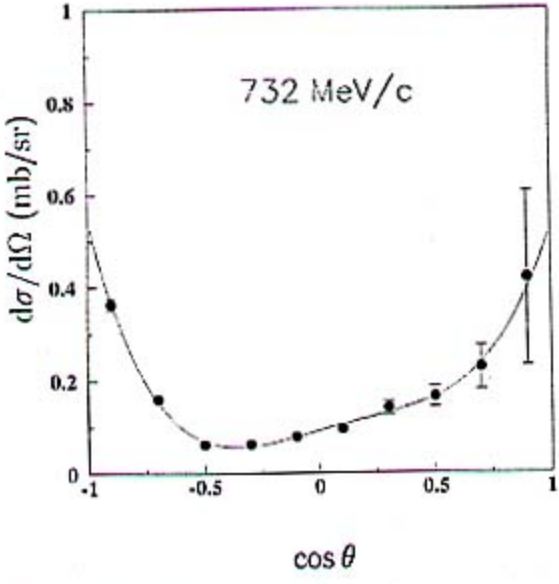

Fig. 4-75: Differential cross section for the reaction $K^-p \to \overline{K^0}n$ at 732 MeV/c.

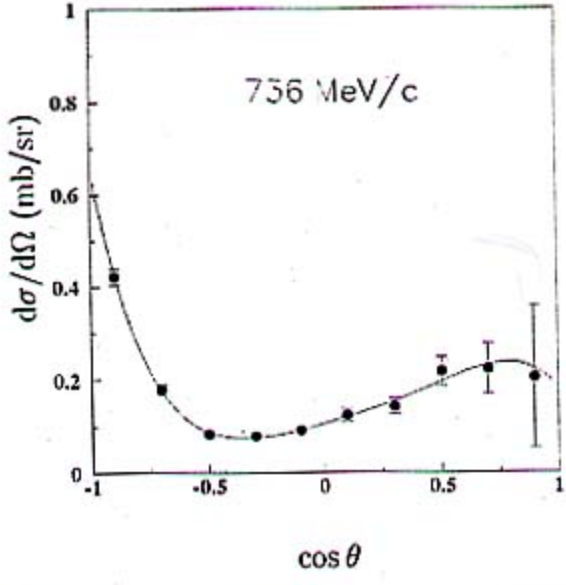

Fig. 4-76: Differential cross section for the reaction $K^-p \to \overline{K^0}n$ at 736 MeV/c.

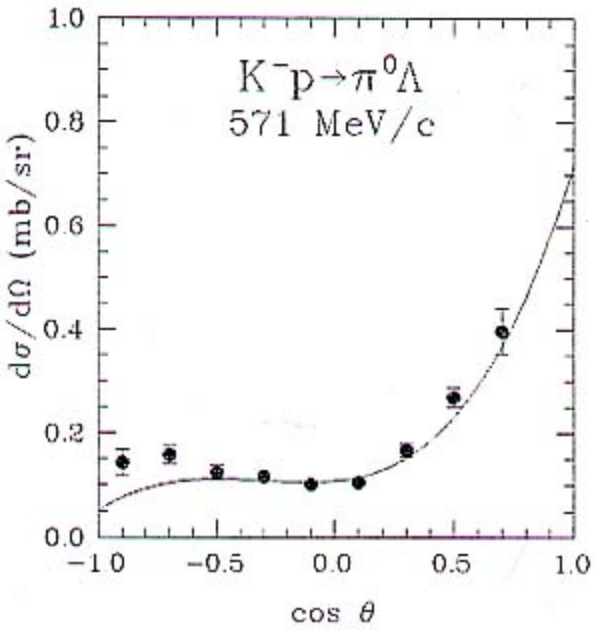

Fig. 4-54: Differential cross section for the reaction $K^-p \to \pi^0\Lambda$ at 571 MeV/c from this analysis compared to partial-wave analysis by Gopal *et al.*

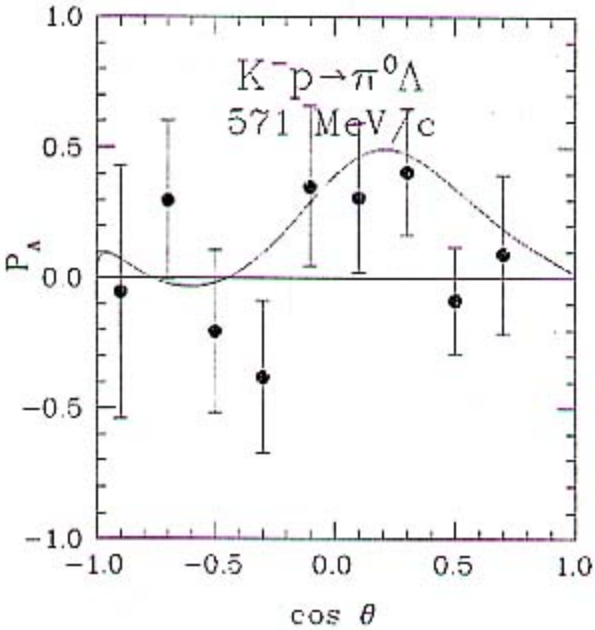

Fig. 4-55: Λ polarization at 571 MeV/c from this analysis compared to partial-wave analysis by Gopal *et al.*

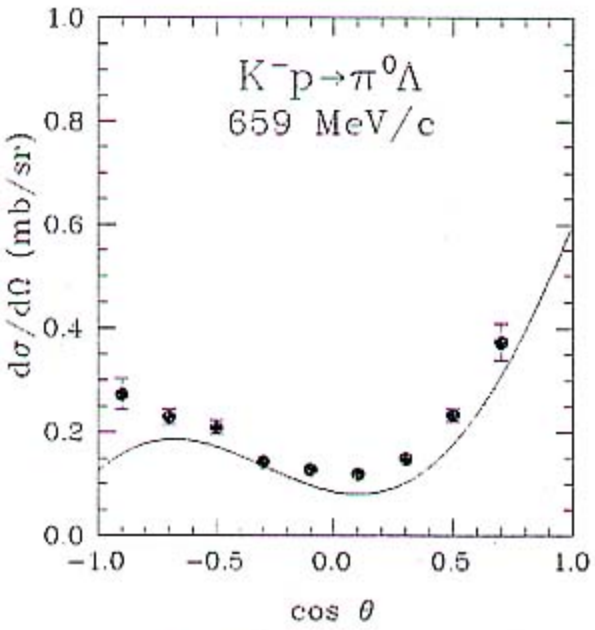

Fig. 4-56: Differential cross section for the reaction $K^-p \to \pi^0\Lambda$ at 659 MeV/c from this analysis compared to partial-wave analysis by Gopal *et al.*

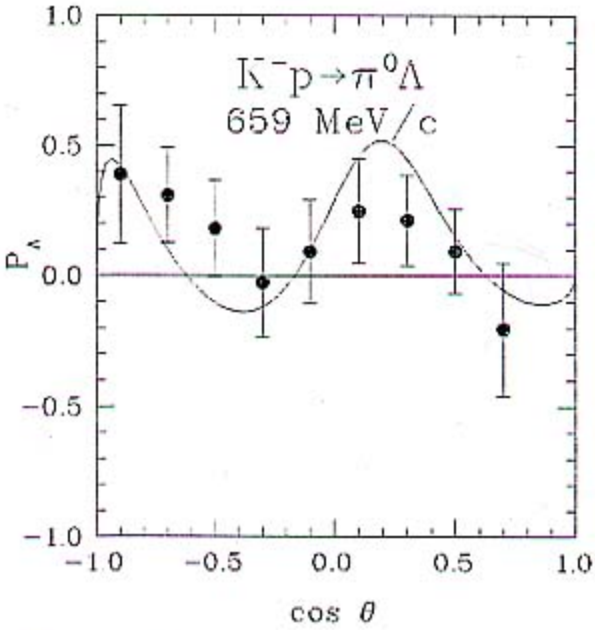

Fig. 4-57: Λ polarization at 659 MeV/c from this analysis compared to partial-wave analysis by Gopal *et al.*

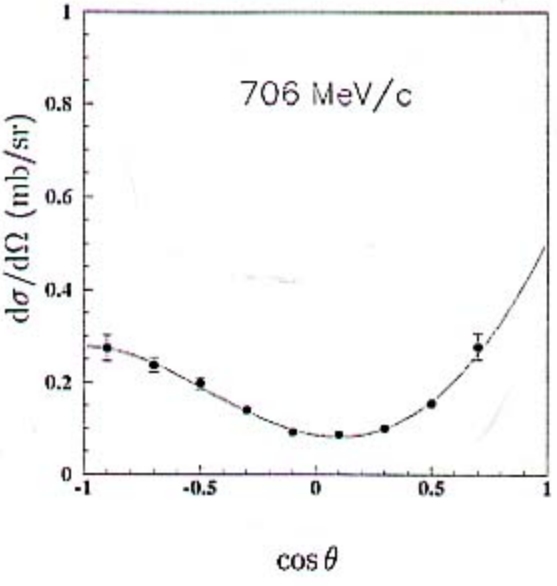

Fig. 4-14: Differential cross section for the reaction $K^-p \to \pi^0\Lambda$ at 706 MeV/c.

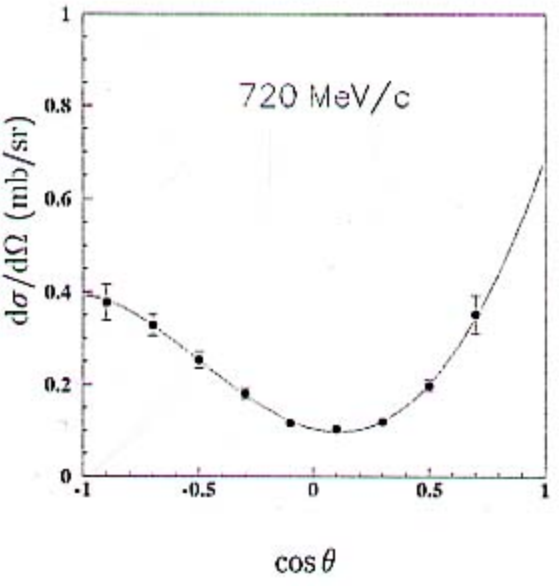

Fig. 4-15: Differential cross section for the reaction $K^-p \to \pi^0\Lambda$ at 720 MeV/c.

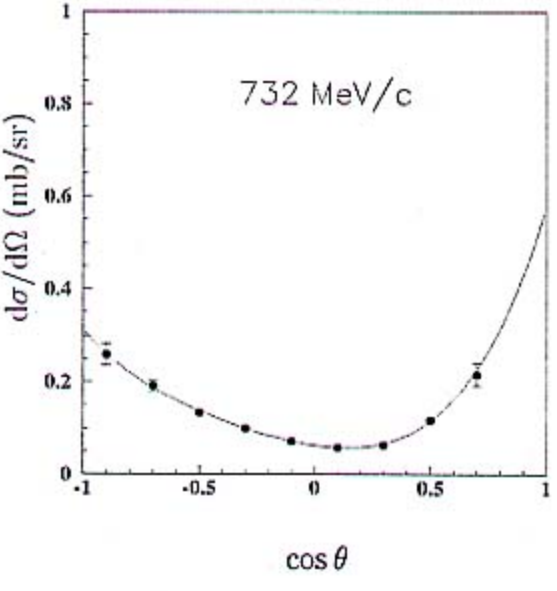

Fig. 4-16: Differential cross section for the reaction $K^-p \to \pi^0\Lambda$ at 732 MeV/c.

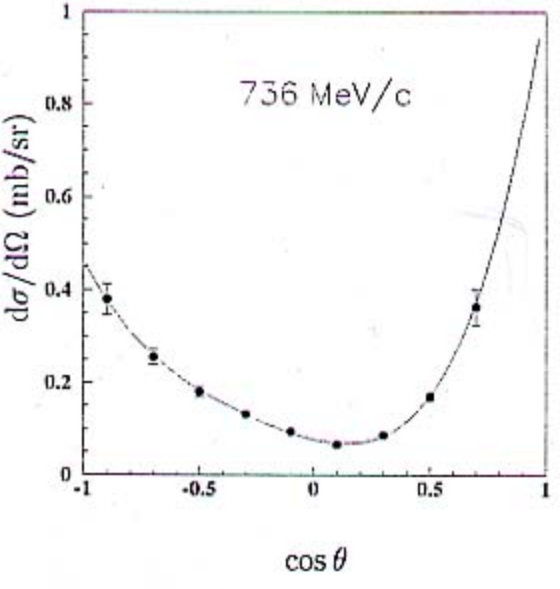

Fig. 4-17: Differential cross section for the reaction $K^-p \to \pi^0\Lambda$ at 736 MeV/c.

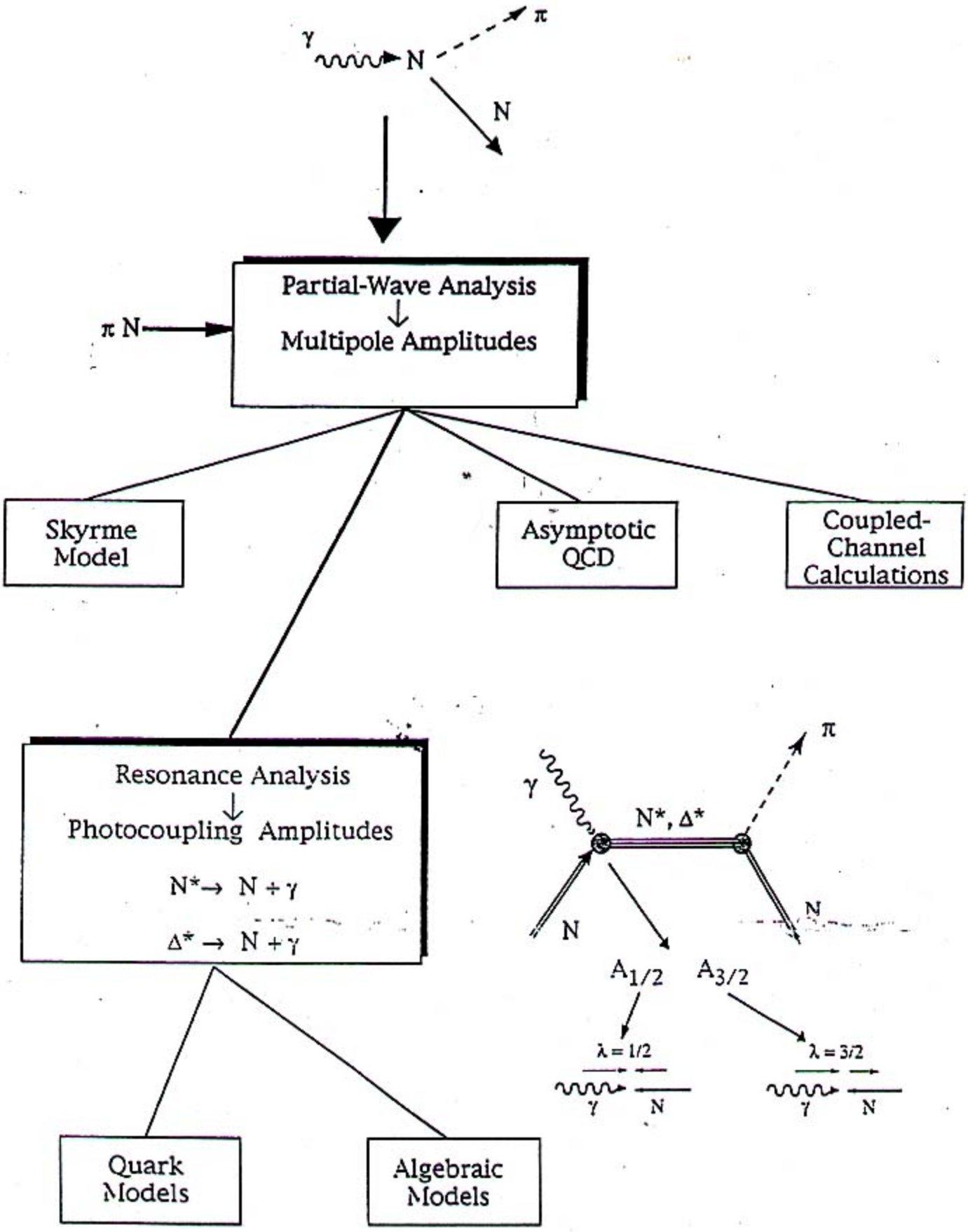
γ
N
π
N
Partial-Wave Analysis
↓
Multipole Amplitudes
π N
Skyrme Model
Asymptotic QCD
Coupled-Channel Calculations
Resonance Analysis
↓
Photocoupling Amplitudes
N* → N + γ
Δ* → N + γ
Quark Models
Algebraic Models
γ
N*, Δ*
π
N
N
A1/2
A3/2
λ = 1/2
λ = 3/2
γ
N
γ
N

Figure 2